

Historic, Archive Document

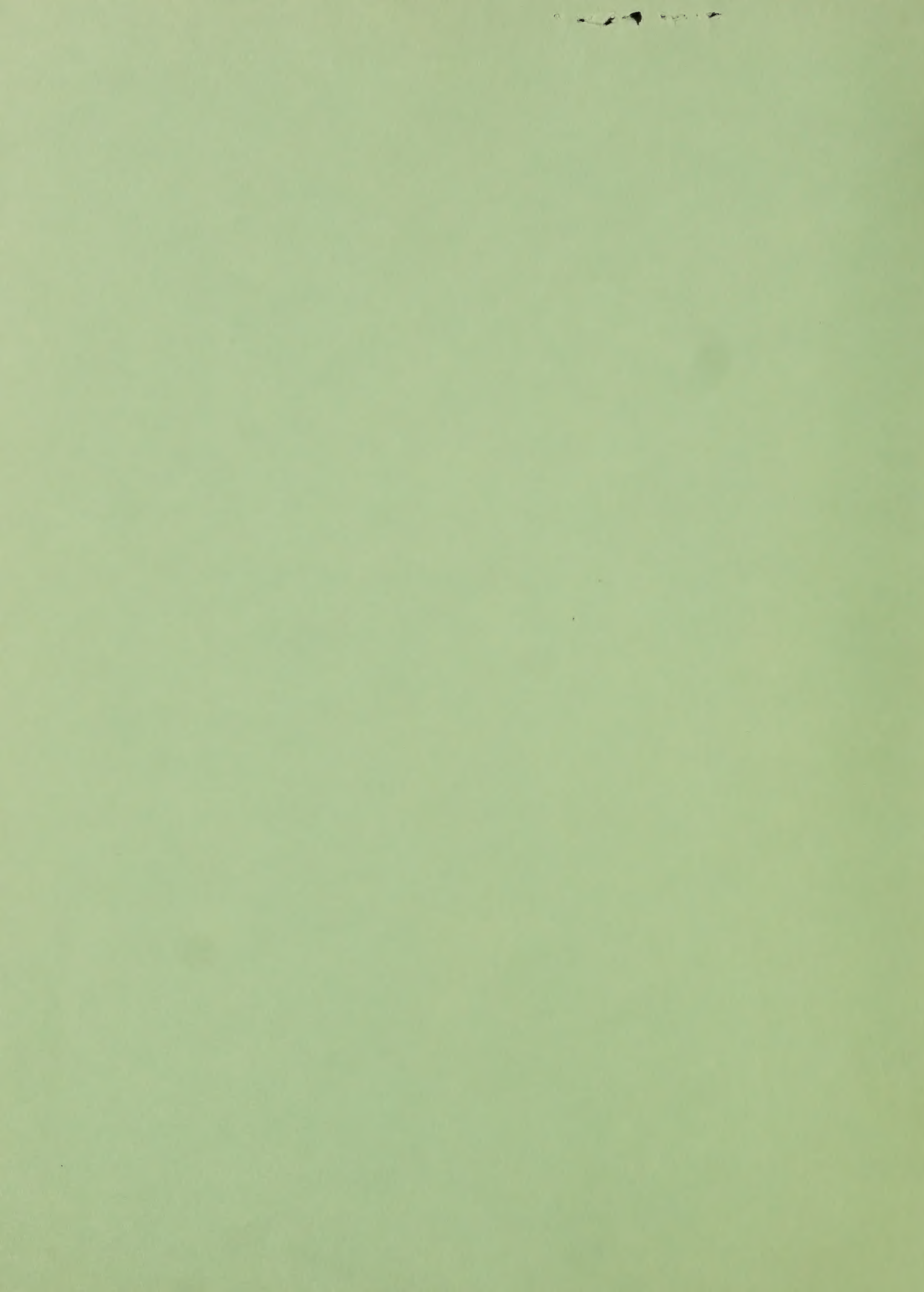
Do not assume content reflects current scientific knowledge, policies, or practices.

Comparison of Modeled and Measured Deposition for the Withlacoochee Spray Trials

*Reporting on the Use of
Aircraft to Apply Pesticides to
Southern Pine Seed Orchards*



**USDA-Forest Service
Forest Pest Management
2810 Chiles Road
Davis, CA. 95616**



FPM 83-1

December 1982

COMPARISON OF MODELED AND MEASURED DEPOSITION FOR
THE WITHLACOOCHEE SPRAY TRIALS

J.E. Rafferty, R.K. Dumbauld,
H.W. Flake, Jr., J.W. Barry and J. Wong

Final Report under Contract No. 53-91S8-9-6260

H.E. Cramer Company, Inc.
University of Utah Research Park
P.O. Box 8049
Salt Lake City, Utah 84108

USDA Forest Service
Forest Pest Management
2810 Chiles Rd.
Davis, California 95616

TABLE OF CONTENTS

<u>Section</u>	<u>Title</u>	<u>Page No.</u>
1	INTRODUCTION	1
	1.1 Background	1
	1.2 Purpose	3
	1.3 Report Organization	3
2	WITHLACOCHEE SPRAY TRIALS	4
	2.1 General	4
	2.2 Deposition Measurements	4
	2.3 Meteorological Measurements	10
	2.4 Aircraft Data	10
3	CBG MODEL INPUTS	12
	3.1 CBG Deposition Model Inputs	12
	3.2 CBG Canopy Penetration Model Inputs	16
4	RESULTS OF THE CALCULATIONS	22
	4.1 Graphs of Observed and Model-Calculated Deposition	22
	4.2 Ratios of Model to Observed Average Deposition Levels	28
5	SUMMARY AND RECOMMENDATIONS	35
	5.1 Summary of Results	35
	5.2 Recommendations	37
	LITERATURE CITED	39
	APPENDIX A	A-1
	APPENDIX B	B-1
	APPENDIX C	C-1

COMPARISON OF MODELED AND MEASURED DEPOSITION FOR THE WITHLACOCHEE SPRAY TRIALS¹

J. E. Rafferty², R. K. Dumbauld²
H. W. Flake, Jr.³, J. W. Barry⁴ and J. Wong⁴

ABSTRACT

The Withlacoochee spray trials were planned and conducted as a pilot project by Southeastern Area-Forest Pest Management (SA-FPM) and FPM-Methods Application Group to evaluate the feasibility of using aerial spray application techniques in the control of cone losses due to coneworm infestations in pine seed orchards. As part of the overall pilot project, deposition measurements were made at the orchard canopy top, within sample trees and on the ground beneath the trees. These measurements were made for use in defining the effectiveness of the aerial spray application technique and to evaluate the potential usefulness of the Cramer-Barry-Grim (CBG) computerized model in the planning, conduct and analysis of seed orchard spray projects. This report describes the Withlacoochee spray trials and compares the deposition measurements with the deposition estimates calculated using the CBG model computer program.

INTRODUCTION

1. Background

The USDA-Forest Service (FS) has been using mathematical models to predict the atmospheric transport, dispersion and deposition of aerially-applied pesticides for more than a decade. Simplified aerial line source models developed for the US Army were applied (GCA Corporation, 1971; H. E. Cramer Company, 1973) early in the decade to determine optimum swath widths and application rates for use in pilot tests of insecticides under consideration at that time for control applications in western forests. The implications of these early efforts in the use of mathematical models to improve the planning, conduct and analysis of spray programs were reviewed in a paper presented at the USFS Workshop for Aerial Application

¹ Prepared for USDA Forest Service, Forest Pest Management, Methods Application Group, Davis, CA under Contract No. 53-91S8-9-6260; John W. Barry, USDA-Forest Service Project Officer.

² H. E. Cramer Company, Inc., P. O. Box 8049, Salt Lake City, UT 84108.

³ USDA Forest Service, SA-FPM, Asheville, NC

⁴ USDA Forest Service, FPM, Davis, CA

of Insecticides Against Forest Defoliators, held in Missoula, Montana, 23-29 April 1974 (Dumbauld, Cramer and Barry, 1975). The H. E. Cramer Company (Dumbauld and Bjorklund, 1977) used aerial spray dispersion models to assist the State of Maine, Bureau of Forestry, in determining offset distances required for various aircraft to ensure that drift from spray blocks in the Maine 1977 spray program posed no environmental hazard to exclusion areas (waterways, homes, etc.) in the vicinity of the spray blocks. Under the sponsorship of the USDA Expanded Douglas-fir-Tussock Moth Research and Development Program, work began in early 1977 on the development of a technical data base for use in applying mathematical dispersion models to FS spray projects and the refinement and adaptation of existing models to predict spray behavior above and within forest canopies. This work (Dumbauld, Rafferty and Bjorklund, 1977) resulted in the development of the CBG computerized spray dispersion model and the comparison of model predictions with measurements made during selected FS spray programs. The CBG computer based model is comprised of two major parts. The first part simulates the deposition of spray drops at the top of a forest canopy. The second part, which is based on a model developed by Grim and Barry (1975), simulates the penetration of spray drops into the forest canopy.

FPM-MAG decided to contract with the H. E. Cramer Company to conduct a joint field effort to demonstrate and advance FS modeling capabilities in predicting requirements for delivering effective doses to target pests and control spray drift beyond target areas. Shortly after work started under the contract, the FPM office at Asheville, NC, proposed a feasibility study of aerial application techniques for the control of seed losses due to seed and cone insects in pine seed orchards. FPM-Asheville and FPM-MAG jointly decided to conduct a pilot project to evaluate aerial application technology for southern seed orchards and to use this pilot project as a field demonstration for the CBG modeling capability. The Withlacoochee State Seed Orchard located near Brooksville, Florida, was selected in December 1979 as the site of the pilot project which was scheduled to be conducted during February 1980. As part of the field demonstration project under Contract No. 53-91S8-9-6260, the H. E. Cramer Company, Inc. used the CBG model to calculate optimum swath widths and release heights for two aircraft types (fixed-wing and helicopter) with spray releases during the early- and late-morning hours at the Withlacoochee State Seed Orchard (Rafferty and Dumbauld, 1980). H. E. Cramer Company personnel also participated in the conduct of the aerial spray trials and were assigned the primary task of assisting the FS in making meteorological measurements required for input to the CBG model.

Aerial pesticide applications to orchards are usually accomplished with aircraft flying immediately above the canopy and calibrated to spray at a rate of from 5 to 10 gallons per acre. Thus, spray strategy differs markedly from that used in spraying western forests where aircraft fly 50 feet above the canopy and apply spray at rates of one gallon or less per acre. The CBG model was developed primarily for use with the latter

strategy and does not incorporate an adequate wake model for use with low-flying aircraft. For this reason close agreement between the model and observed spray deposition pattern was not expected, but the opportunity to develop a data base for future application of the CBG model to seed orchard spray activities was welcomed.

1.2 Purpose

The purpose of this report is to describe the final phase of the field demonstration of the CBG model. The major topics discussed in the report are a comparison of model deposition estimates with deposition measurements made during the Withlacoochee spray trials and an overall evaluation of the usefulness of the model in planning and conducting orchard spray projects.

1.3 Report Organization

Section 2 contains a general description of the Withlacoochee spray trials. The inputs required by the CBG model for dispersion, deposition and canopy penetration calculations and the values assigned to these inputs are described in Section 3. Section 4 contains a description of the procedures used in the model calculations and a comparison of the results of the model calculations with the measurements made during the spray trials. The results are summarized in Section 5 which also contains recommendations for further study of the trial data and for model improvements. A brief description of the model used in this study is provided in Appendix A. Appendix B contains drop-size distribution data for the selected trials used in the comparison of model deposition estimates with deposition measurements. Appendix C presents graphs of observed and model deposition patterns for selected trials.

SECTION 2 WITHLACOOCHEE SPRAY TRIALS

2.1 General

The Withlacoochee State Seed Orchard is located a few miles north and west from the intersection of Highway 98 and Interstate 75 near Brooksville, Florida. The surrounding terrain is gently rolling with elevations varying between 50 and 150 feet (15.2 and 46 meters) above mean sea-level within 1 mile (1.61 kilometers) from the spray trial site and a maximum elevation of 261 feet (80 meters) occurring at Munden Hill, 3 miles (4.8 kilometers) west-southwest from the spray trial site. The orchard contains stands of slash pine and Ocala sand pine, some of which are stunted and poorly formed because of poor soil and drainage conditions. For the purposes of the spray trials, an area on the east side of the orchard containing relatively uniform stands of slash and Ocala sand pine was selected. Figure 2-1 is a schematic diagram of a portion of the selected area. The trees are planted every 15 feet (4.5 meters) in north-south rows separated by a distance of 30 feet (9.1 meters). As shown in the figure, slash pine is planted north of the 45-foot (14-meter) service road and Ocala sand pine is planted south of the road. The locations of the sample trees within which detailed deposition measurements were made are indicated by the numbers 1 through 12. Eight of the sample trees were located in the slash pine orchard and four were located in the more dense Ocala sand pine orchard. A limited survey of the trees in the vicinity of the sample trees in the slash pine was made to locate undersized and missing trees. In the schematic diagram the larger open circles represent typical trees and the smaller open circles represent undersized or thinly branched trees. The absence of a tree is shown by a cross symbol (+). The rows of trees in every case extended about 1200 feet (366 meters) to the north and south of the service road shown in the diagram. .

There were 12 aircraft spray trials conducted during the study. As shown in Table 2-1, a modified Stearman fixed-wing aircraft was used in 7 trials and a Hughes 500C helicopter was used in 5 trials. On each trial the aircraft flew north and south along the rows or between the rows (see Section 3). Except for Trial 14, water containing Nalco-Trol and Rhodamine B liquid dye was released on each trial. Nalco-Trol was not added to the spray mix on Trial 14. Manganese sulfate was added to the tank mix on Trials 5, 6, 7 and 10 so a mass deposit analysis of samples could be performed.

2.2 Deposition Measurements

As noted above, deposition measurements were made at the top of the canopy, within the canopy and at the ground beneath the canopy. Measurements at the top of the canopy and within the canopy were made using empty aluminum soft-drink cans wrapped on the sides with Kromekote card material (4 1/4 inches by 8 3/16 inches) and with a 2 1/2-inch diameter

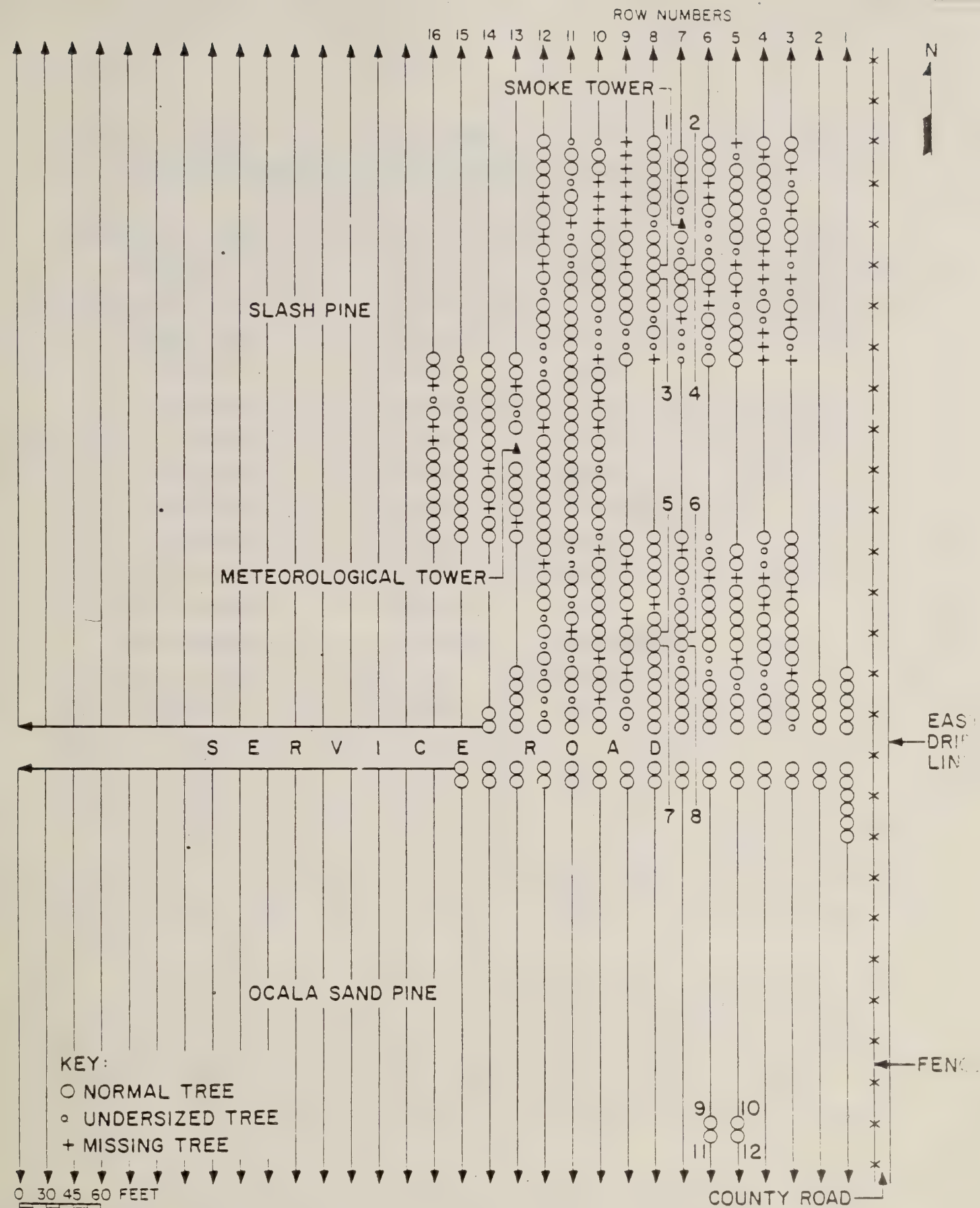


FIGURE 2-1. Schematic diagram of the test area, Withlacoochee State Seed Orchard, Florida, 1980.

TABLE 2-1
DATES, TIMES AND AIRCRAFT TYPE FOR THE WITHLACOOCHEE STATE
SEED ORCHARD TRIALS

Trial Number	Date (1980)	Time (EST)	Aircraft Type
1	13 Feb	1554:37	Stearman
2	15 Feb	1007:30	Stearman
3	15 Feb	1506:40	Stearman
5	16 Feb	1214:20	Stearman
6	16 Feb	1632:35	Stearman
7	18 Feb	0942:24	Stearman
8	19 Feb	0734:15	Stearman
10	19 Feb	1707:23	Hughes 500 C
11	20 Feb	0748:05	Hughes 500 C
12	20 Feb	1043:05	Hughes 500 C
13	20 Feb	1756:54	Hughes 500 C
14	21 Feb	0749:21	Hughes 500 C

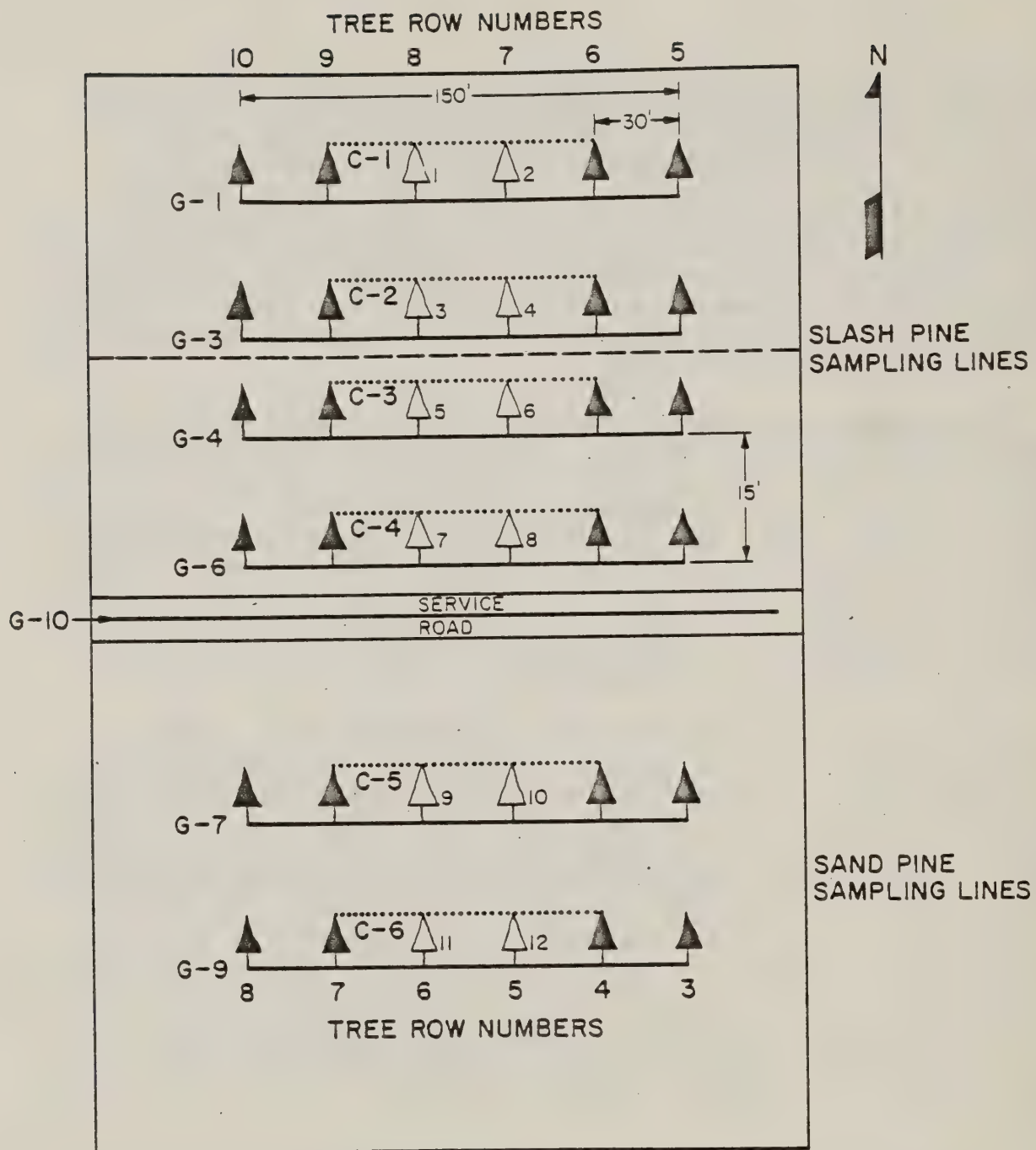
circle of Kromekote card material taped to the top of the can. At the top of the canopy, the cans were suspended from a line stretched east-west across the tree rows at the position of the sampling trees. As shown in Figure 2-2 by the dotted lines, the canopy sampling lines extended one row east and west of the sample trees and the cans were suspended at intervals of 6 feet (1.8 meters) along each line. The Kromekote-wrapped cans were also placed within the canopy on the sampling trees in the upper crown, mid-crown and in the lower crown at the four cardinal directions (north, east, south and west) for a total of 12 cans per sampling tree. In each case, the cans were suspended from the ends of branches to simulate pine cones.

Ground-level measurements were made using 6 11/16-by 4 5/16-inch Kromekote cards in plastic holders. Ground-sampling lines were placed beneath the sampling trees as shown in Figure 2-2 by the solid lines and extended two tree rows east and west of the sample trees. Cards were placed at intervals of 3 feet (0.9 meters) along these ground-sampling lines. Ground measurements using the Kromekote cards in plastic holders were also made along the middle of the service road between the slash pine and Ocala sand pine stands at 10-foot (3-meter) intervals. The service road sampling line began at row 1 in Figure 2-1 and extended westward for about 650 feet (198 meters).

Drift measurements were made using Kromekote cards in plastic holders and wrapped soft-drink cans. Depending on the wind direction for a given trial, drift samplers were placed along lines to the north, east, south or west of the aircraft spray lines. The east drift line is shown in Figure 2-1. The north and south drift lines were about 1,312 feet (400 meters) north and south of the service road shown in Figure 2-1, just beyond the end of the tree rows in the orchard. The west drift line was located about 1,312 feet (400 meters) west of tree row number 1. If the wind direction for a trial was from, for example, the southwest or south, samplers were placed along the north and east drift lines. The cards in plastic holders were placed at 100-foot (30.5-meter) intervals along the spray drift sampling line and wrapped soft-drink cans were placed at 200-foot (61-meter) intervals on top of 3-foot (1-meter) wood stakes.

As mentioned above, manganese sulfate was added to the aircraft tank mix on Trials 5, 6, 7 and 10 so that atomic absorption techniques could be used to obtain direct estimates of mass deposition. Mylar sheeting and Kromekote cards were used for subsequent mass analysis at selected locations in the ground-sampling network, on all tree soft-drink can samplers at 6-foot (1.8 meter) intervals along the canopy lines, and at every other sampling location on the drift sampling lines for these trials.

Not all ground samplers, tree samplers, and top-of-canopy samplers were used in all trials because of the time required to put the samplers in place. Table 2-2 shows the ground sampling rows and canopy-top sampling rows (refer to Figure 2-2 for locations) used in the comparisons



— GROUND SAMPLING LINE - samplers every 3 feet
 CANOPY SAMPLING ARRAY - samplers every 6 feet

▲ SAMPLING TREE

▲ NON-SAMPLING TREE

FIGURE 2-2. Sampling array for Withlacoochee State Seed Orchard trials, Florida, 1980.

TABLE 2-2
SAMPLING DATA USED IN THE COMPARISON OF MODEL DEPOSITION
ESTIMATES AND DEPOSITION MEASUREMENTS

Trial Number	Ground Rows							Canopy-Top Rows					
	G-1	G-3	G-4	G-6	G-7	G-9	G-10	C-1	C-2	C-3	C-4	C-5	C-6
2	X	X	X	X	X	X	X	X	X	X	X	X	X
3	X	X	X	X	X	X	X	X	X	X	X	X	X
5	X	X	X	X	X	X	X	X	X	X	X	X	X
6	X	X	X	X	X	X	X	X	X				
7	X	X	X	X	X	X	X	X	X	X	X	X	X
10	X	X			X	X	X	X	X			X	X
11	X	X			X	X	X	X	X			X	X
13	X	X			X	X	X	X	X			X	X

TABLE 2-3
AIRCRAFT DATA

Aircraft	Speed ($m s^{-1}$)	Weight (kg)	Wing or Rotor Span (m)	Type of Nozzles*	No. of Nozzles	Boom Pressure (psig)
Stearman	40	1406	11.48	D6-46	27	40
Hughes 500 C	11-14	1157	8.03	D2-45	22	40

*Spraying Systems Co.

of model deposition estimates with deposition measurements presented in Section 4.

2.3 Meteorological Measurements

Meteorological measurements were made on a 52-foot (16-meter) tower located on tree row number 13 at the position shown in Figure 2-1. MRI Vectorvanes were mounted at heights of 6.6 and 52.5 feet (2 and 16 meters) on the meteorological tower. The Vectorvanes measured azimuth and vertical wind directions and wind speed which were recorded on Esterline Angus strip-chart recorders located at the base of the tower. A Climatronics Electronic Weather Station was used to measure and record azimuth wind direction and wind speed at a height of 6.6 feet (2 meters) at a position in an open field about 1480 feet (450 meters) west of the tree row number 1 and about 66 feet (20 meters) south of the service road. Wind direction, wind speed, temperature and relative humidity measurements were made to heights of 230 feet (70 meters) during most trials using a Tethersonde. The Tethersonde was located about 810 feet (247 meters) west of tree row number 1 and 141 feet (43 meters) south of the service road in a small open area.

2.4 Aircraft Data

Table 2-3 shows the approximate airspeeds and weights of the aircraft used in the trials, the aircraft wing or rotor span, and the type and number of nozzles used in the spray trials. The spray boom was mounted immediately aft of the lower wing on the Stearman. The spray boom on the Hughes 500 C helicopter was mounted a few feet below the fuselage about midway between the front and rear landing skid struts. Table 2-4 shows the gallons of material sprayed on each trial, the nominal aircraft flight altitude above the top of the canopy, and the position of the aircraft swaths flown on each trial with respect to the tree row numbers shown in Figure 2-1.

TABLE 2-4
POSITION OF AIRCRAFT SWATHS WITH RESPECT TO TREE ROWS
AND GALLONS SPRAYED

Trial Number	Aircraft Type	Gallons Sprayed	Flight Altitude Above Canopy (m)	Tree Row							
				1	2	3	4	5	6	7	8
2	Stearman	80	5.74								
3	Stearman	77	5.74								
5 ②	Stearman	83	1.52								
6	Stearman	65	1.52								
7	Stearman	15	1.52								
10 ②	Hughes 500 C	92	1.52								
11	Hughes 500 C	100	1.52								
13	Hughes 500 C	100	1.52								

① The crosses on the lines between tree rows indicates the aircraft flew between the tree rows.

② Double crosses (XX) indicate the aircraft flew twice over these positions.

SECTION 3 CBG MODEL INPUTS

The model inputs required in the CBG model calculations are described in this section. The CBG deposition model, used to calculate the deposition at the top of the slash and Ocala sand pine canopy, and the CBG canopy penetration model, used to calculate deposition within and below the canopy, are described in Appendix A.

3.1 CBG Deposition Model Inputs

3.1.1 Meteorological Inputs

The meteorological inputs required by the deposition model are listed in Table 3-1. The wind speed \bar{u}_R , the mean above-canopy wind direction θ , and the standard deviations $\sigma_A\{\tau_0\}$ and σ_E used in the deposition model calculations were obtained from the MRI Vectorvane measurements made at a height of 52.5 feet (16 meters) on the meteorological tower located at the position shown in Figure 2-1. The Vectorvanes were about 13 feet (4 meters) above the surrounding tops of the slash pines. The Esterline Angus strip charts recorded the wind-speed and azimuth and vertical wind directions starting 1 minute before the aircraft began spraying the tree rows until 5 minutes after the last row was sprayed. On the average, the total data record length for each trial was about 12 minutes for the Stearman aircraft trials and about 22 minutes for the Hughes 500 C trials because of the lower air speed of the Hughes 500 C and the need for refilling the spray tanks of this aircraft during each trial. The wind speed and the azimuth and vertical wind directions were read from the chart records at 4-second intervals. The mean wind speed, azimuth wind direction and the standard deviations were calculated from the 4-second data records for the first continuous 10-minute period of the record after spraying began that did not contain any calm wind conditions or missing data. For the eight trials used in the comparison of model calculations and measured deposition, the maximum time offset for the start of this period was 2.2 minutes after spraying began, which occurred on Trial 10. The meteorological deposition model inputs for the eight trials derived from the Vectorvane data are shown in Table 3-2.

Values of the wind profile power-law exponent p were set equal to zero in the deposition model calculations because the aircraft never flew at altitudes greater than 19 feet (5.74 meters) above the canopy and we believe the data from the top of the meteorological tower best represent conditions affecting deposition at the canopy top. The depth of the surface mixing layer H_m is important in deposition calculations when the spray material has relatively small settling velocities and either the spray material is released above an inversion, or below a capping inversion and deposition is calculated at intermediate and long travel distances downwind from the aircraft flight paths. Because the aircraft

TABLE 3-1
METEOROLOGICAL INPUT PARAMETERS
REQUIRED BY THE DEPOSITION MODEL

Parameter	Parameter Definition
$\sigma_A \{\tau_0\}$	Standard deviation of the wind azimuth angle (deg) for the averaging time τ_0
σ_E	Standard deviation of the wind elevation angle (deg)
H_m	Depth of the surface mixing layer below a capping inversion (m)
$\bar{u}_R \{z_R\}$	Wind speed at a reference height z_R ($m s^{-1}$)
p	Wind speed profile power-law exponent
θ	Mean above-canopy wind direction (deg)

TABLE 3-2
METEOROLOGICAL INPUTS TO THE CBG DEPOSITION MODEL

Trial Number	$\sigma_A \{\tau_0 = 10 \text{ min}\}$ (deg)	σ_E (deg)	$\bar{u}_R \{z_R = 16 \text{ m}\}$ ($m s^{-1}$)	θ (deg)
2	14.1	11.7	1.02	23
3	14.9	22.4	1.10	20
5	16.2	12.0	3.15	214
6	15.2	9.9	4.21	256
7	27.0	19.4	6.20	33
10	19.6	14.6	1.76	360
11	5.7	5.6	.94	305
13	16.6	12.7	1.90	265

flew just above the canopy and because the gravitational settling velocities and aircraft wake settling velocities were significant, the presence of an inversion in the vicinity of the canopy would have little effect on the deposition. Also, the Tethersonde measurements indicated that there were no inversions below a height of 200 feet (60 meters) except for Trial 11, when a surface based inversion was present. For these reasons a value of 1000 meters was assigned to H' for all trials to preclude the reflection of drops from capping inversions in the deposition calculations.

3.1.2 Source Model Inputs

The source model inputs required by the deposition model are defined in Table 3-3. The values of Q , H' , σ_0 and L used in the deposition model calculations are shown in Table 3-4. The source strengths for each trial in Table 3-4 were calculated from the expression

$$Q(\text{gm}^{-1}) = \left(\frac{Q_T}{L \cdot n} \right) \left(\frac{3.78501 \cdot 10^3 \text{g}}{\text{gallon}} \right) \quad (3-1)$$

where

Q_T = Total gallons sprayed (see Table 2-4)

n = Number of tree rows sprayed (see Table 2-4)

In previous studies (Dumbauld, Rafferty and Bjorklund, 1977) the effective release height H' has been calculated using an expression accounting for the effects of wake turbulence, which cause the spray cloud to sink to a height of one-half wing span or rotor diameter ($b/2$) above the canopy. However, because the flight altitudes were at or below the height ($b/2$) in the Withlacoochee Spray Trials, the effective release heights H' were set equal to the aircraft flight altitude H above the top of the canopy. The height ($b/2$) is also generally used to determine the initial source dimensions σ_0 from the expression

$$\sigma_0 \{x_R\} = \frac{H - (b/2)}{2.15} \quad (3-2)$$

Because the numerator of Equation (3-2) would be negative for the Withlacoochee Spray Trials, the following dimensions were arbitrarily assigned at the source location ($x_R = 0$):

TABLE 3-3
SOURCE INPUT PARAMETERS REQUIRED BY THE DEPOSITION MODEL

Parameter	Definition
Q	Source strength (g m^{-1})
H'	Effective height of the spray cloud release (m)
$\sigma_0 \{x_R\}$	Standard deviation of the cloud distribution at the distance x_R from the source (m)
L	Length of line source (m)
f_j	Fraction of the total source strength in the j^{th} drop-size category
v_j	Gravitational settling velocity for the median drop by mass in the j^{th} drop-size category (m s^{-1})
γ_j	Reflection coefficient for the median drop by mass in the j^{th} drop-size category

TABLE 3-4
INPUT VALUES OF Q , H' , σ_0 AND L USED IN
THE CBG DEPOSITION MODEL CALCULATIONS

Trial Number	Q (g m^{-1})	H' (m)	$\sigma_0 \{x_R = 0\}$ (m)	L (m)
2	57.33	5.74	4.00	754.6
3	48.28	5.74	4.00	754.6
5	46.26	1.52	2.67	754.6
6	36.23	1.52	2.67	754.6
7	8.36	1.52	2.67	754.6
10	46.15	1.52	1.87	754.6
11	55.74	1.52	1.87	754.6
13	55.74	1.52	1.87	754.6

$$\begin{aligned}
 1.5 \frac{b}{4.3} ; H' &= 5.74 \text{ m} \\
 \sigma_0 &= \\
 b/4.3 ; H' &= 1.52 \text{ m}
 \end{aligned} \tag{3-3}$$

The length of each tree row (2476 feet or 754.6 meters) was assigned to the line length L used in Equation (3-1) above.

The drop-size distributions for use in the deposition model calculations were obtained from the drop-size distributions calculated from the deposition measurements made on the Kromekote card samplers placed on the ground sampling row G-10 located on the service road between the slash and Ocala sand pine stands. Briefly, the drop-size distributions were obtained by the FS using a Quantimet Image Analyzer and their ASCAS (Automatic Spot Counting and Sizing) data program. The image analyzer counts the stains produced by the dyed spray drops and measures drop-stain diameters on a representative area of the sampling card in up to 16 pre-selected size categories. The ASCAS program uses the counts in the 16 size categories, a mathematical equation relating stain diameters to actual drop diameter, and the drop density (1 g cm^{-3} , in this case) to produce the mass distribution measured on a sampling card or group of cards. Table 3-5 contains the values of f_j , V_j and γ_j assigned to the drop-size categories measured for Trial 2. Similar information for all eight trials used in this study is contained in Appendix B. The values of f_j were obtained directly from drop-size distribution information produced by the ASCAS program. Values of the gravitational settling velocity V_j were calculated for drops of unit density and the mean drop diameters for each category using the technique described by McDonald (1960). The values of the reflection coefficient γ_j shown in the table are based on the relationship between gravitational settling velocities and reflection coefficients postulated by Dumbauld, Rafferty and Cramer (1976). A value for γ_j of 0 means the drops in this category are deposited at the ground or, for deposition calculations at the canopy top, that all drops in the category enter the top of the canopy. A value of 1 for γ_j means that all drops are reflected at the canopy top or at the ground. The value for γ_j of 0.59 in Table 3-5 for the first drop-size category means that 59 percent of the drops reaching the canopy top are reflected and 41 percent enter the canopy.

3.2 CBG Canopy Penetration Model Inputs

3.2.1 Meteorological Model Inputs

The mean wind speeds in quarters of the forest canopy are the only meteorological inputs required by the canopy penetration model. Although

TABLE 3-5
 DROP-SIZE DISTRIBUTION, SETTLING VELOCITIES v_j AND
 REFLECTION COEFFICIENTS γ_j FOR TRIAL 2 OF THE
 WITHLACOOCHEE SPRAY TRIALS

Drop-Size Category j	Mean Drop Diameter (μm)	f_j	v_j (m s^{-1})	γ_j
1	38.0	0.001	0.0629	0.59
2	78.3	0.009	0.216	0.21
3	118.0	0.02	0.402	0
4	153.0	0.03	0.595	0
5	185.0	0.04	0.741	0
6	228.0	0.10	0.926	0
7	278.0	0.10	1.20	0
8	327.0	0.10	1.44	0
9	406.0	0.20	1.76	0
10	486.0	0.10	2.07	0
11	546.0	0.10	2.36	0
12	623.0	0.10	2.73	0
13	705.0	0.04	3.11	0
14	792.0	0.03	3.44	0
15	933.0	0.02	3.96	0
16	1231.0	0.01	4.93	0

as mentioned in Section 2, a Vectorvane was located at a height of 6.6 feet (2 meters) on the meteorological tower, the wind speeds within the canopy were usually so light and variable that the accuracy of the measurements was questionable. For this reason, we used the normalized wind profile given by Fritschen, *et al.* (1970) for an isolated conifer stand of similar stem density with no understory to define the below-canopy wind profile. The below-canopy wind speeds in Table 3-6 were obtained by assuming that the wind speed measured at the top of the meteorological tower was equivalent to the value indicated by the Fritschen profile at the canopy top. The wind speeds in Table 3-6 were used in calculating the deposition below the canopy described in Section 4.

3.2.2 Canopy Inputs

The canopy penetration model requires the canopy data inputs and related information described in Table 3-7. The values used in the canopy penetration model calculations for this study for H_c , D_t , PRPEN and M are given in Table 3-8. Tree widths are given in Table 3-9. The average tree widths and heights were determined from measurements of the sample trees made during the trials. The values of PRPEN were based on estimates provided by Grim and Barry (1975) for conifer trees with moderate (their foliage type III for the slash pine) and heavy (their foliage type IV for the Ocala sand pine) foliage densities. The impaction collection efficiencies for the canopy penetration calculations were calculated from the following empirical relationship, recommended by Grim and Barry (1975) and attributed to Sell:

$$E_j = \begin{cases} \frac{2.8 \times 10^{-4} d_j^2 u}{s} & ; \quad E_j \leq 1 \\ 1 & ; \quad E_j > 1 \end{cases} \quad (3-4)$$

where

u = impaction velocity in meters per second

d_j = drop diameter for the j^{th} category in micrometers

s = diameter in centimeters of the element on which the drop impacts

Grim and Barry obtained a good fit to their deposition data using a value for s of 13 centimeters. We have also used this value of s in model calculations made for the Rennic Creek Trials (see Dumbauld, Rafferty and Bjorklund, 1977). The impaction velocity u in Equation (3-4) was set equal to the mean wind speed in the forest canopy obtained by averaging the four values for each trial shown in Table 3-6. Values of E_j for each drop-size category are shown for each trial in the tables contained in Appendix B.

TABLE 3-6
MEAN WIND SPEEDS IN METERS PER SECOND USED IN THE CANOPY PENETRATION MODEL CALCULATIONS

Trial Number	Canopy Height Interval (k)			
	1 (Base)	2	3	4 (Top)
2	0.95	0.84	0.82	0.90
3	1.02	0.90	0.88	0.97
5	2.93	2.58	2.52	2.77
6	3.92	3.45	3.37	3.70
7	5.74	5.06	4.94	5.43
10	1.64	1.44	1.41	1.55
11	0.87	0.77	0.75	0.83
13	1.77	1.56	1.52	1.67

TABLE 3-7
CANOPY RELATED INPUTS REQUIRED BY THE
CANOPY PENETRATION MODEL

Parameter	Description
H_c	Tree height (m)
D_t	Tree density (stems per acre)
PRPEN	Probability of penetration
M	Total number of drops to be passed along the trajectory
w_i	Tree width at one-meter height intervals (m)
E_j	Impaction collection efficiency for the j^{th} drop-size category

TABLE 3-8
VALUES OF CANOPY RELATED INPUTS USED IN THE
CANOPY PENETRATION CALCULATIONS

Parameter	Value	
	Slash Pine	Ocala Sand Pine
H_c (m)	12	14
D_t (stems/acre)	96.8	96.8
PRPEN	0.38	0.13
M (drops)	1000	1000

TABLE 3-9
TREE WIDTHS FOR THE SLASH
AND OCALA SAND PINES

Tree Height (m)	Tree Width (m)	
	Slash Pine	Ocala Sand Pine
1	.21	.31
2	.19	.30
3	.19	.30
4	3.8	7.2
5	6.6	7.1
6	6.2	7.8
7	5.8	7.1
8	5.4	6.4
9	5.0	6.1
10	4.0	5.9
11	3.3	5.4
12	1.6	4.4
13		3.0
14		1.5

SECTION 4
RESULTS OF THE CALCULATIONS

The model inputs described in Section 3 were used in the line-source deposition model presented in Appendix A to calculate deposition at the canopy top along sampling rows C-1 through C-6 (see Figure 2-2). Deposition calculations along the ground-level sampling rows G-1 through G-9 were made using the canopy-penetration model described in Appendix A. The results of these calculations and comparisons of these results with observed deposition are described below.

4.1 Graphs of Observed and Model-Calculated Deposition

Graphs of observed and model-calculated deposition at the top of the slash pine canopy and on the ground beneath the canopy for all trials are presented in Appendix C. Figure 4-1 shows the observed and model deposition at the canopy top for Trial 2 in which the Stearman aircraft flew at a height of 19 feet (5.74 meters) above the canopy. In Figure 4-1, downline distance is measured from west to east along the sampling rows C-1 through C-4. The observed deposition plotted in the figure is the arithmetic average deposition at the sampler positions located at the same downline distances. For example, the observed deposition values at samplers C-1-1, C-2-1, C-3-1 and C-4-1 were summed and divided by 4 to obtain the deposition plotted at the downline distance of 0. The model deposition values shown in Figure 4-1 are also average deposition values at each downline distance.

Inspection of Figure 4-1 shows that the peak depositions along the sampling rows predicted by the model are greater than the observed peaks and the model depositions in the troughs are much smaller than the observed depositions in the troughs. The peaks in the model and observed deposition pattern reflect the maximum deposition at the top of the canopy from individual swaths of the Stearman aircraft. Our experience in modeling aircraft spray deposition patterns indicates that the ratio between the model depositions for the peaks and troughs is principally controlled by the value assigned to the source dimension σ_0 at the height of cloud stabilization above the canopy. In previous comparisons of observed and model-calculated deposition patterns for aircraft flying at several wingspans above the top of the canopy (Dumbauld, Rafferty and Cramer, 1976; Dumbauld, Rafferty and Bjorklund, 1977), the use of Equation (3-2) to determine σ_0 yielded satisfactory agreement between the observed and model-calculated peaks and troughs in the deposition pattern. As noted in Section 3.1.2 above, Equation (3-2) is based on aircraft wake effects and could not be used for the Withlacoochee Spray Trials because the aircraft flight altitudes were less than half a wing span or rotor diameter above the canopy. Therefore we used an arbitrary expression for σ_0 given by Equation (3-3). The effects of doubling the value of σ_0 assigned on the basis of Equation (3-3) for the Trial 2 model calcula-

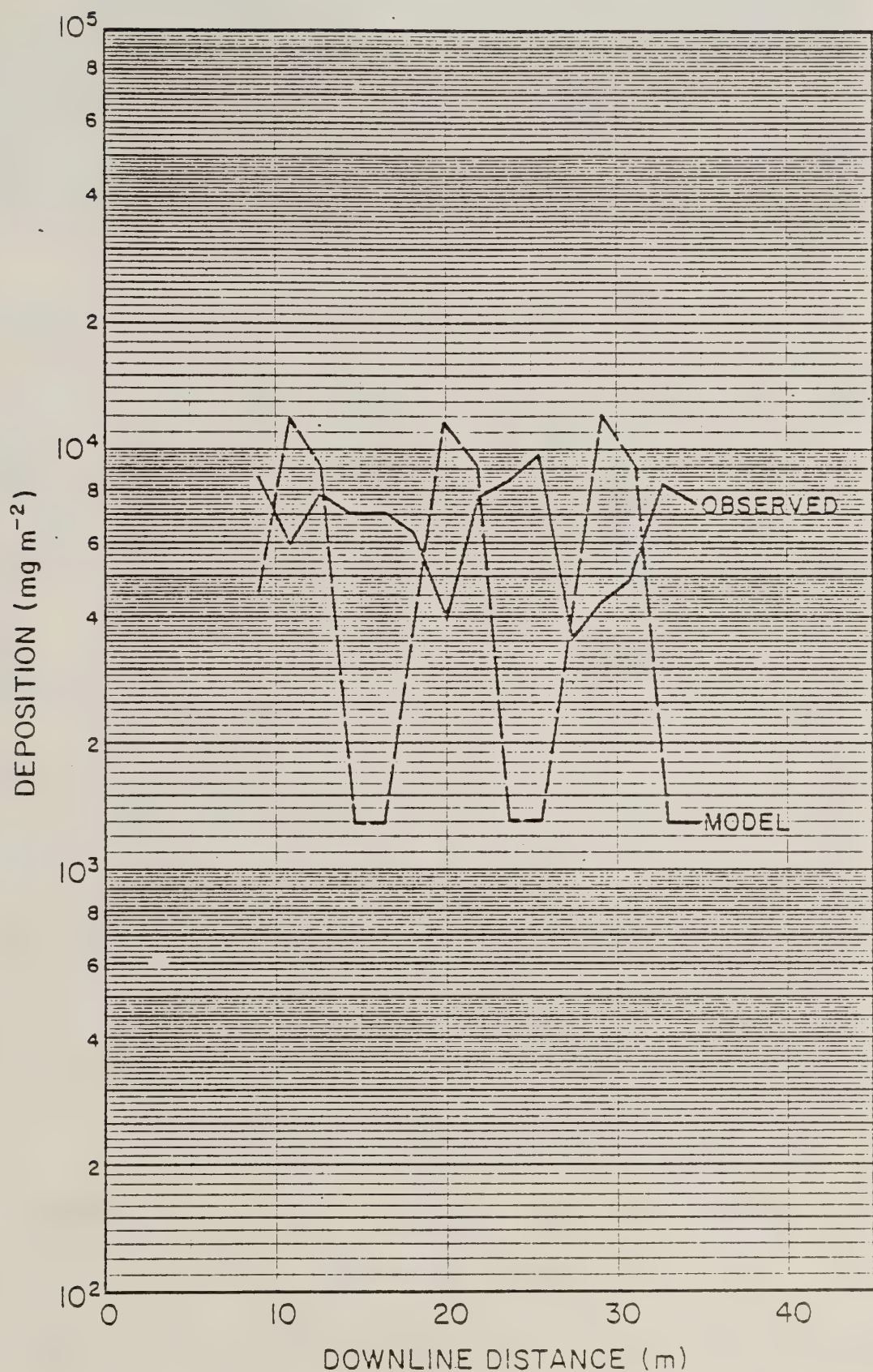


FIGURE 4-1. Observed and model deposition at the top of the slash pine canopy for Trial 2, Withlacoochee Spray Trials, Florida, 1980.

tions are illustrated in Figure 4-2. Comparison of Figures 4-1 and 4-2 shows that doubling the value of σ_0 produces a model deposition pattern more nearly reflecting the peak-to-trough ratio in the observed deposition pattern. The doubling of σ_0 also increases the average calculated deposition level along the downline distance from 3.61×10^3 to $4.75 \times 10^3 \text{ mg m}^{-2}$, as compared to the average observed deposition level of $5.12 \times 10^3 \text{ mg m}^{-2}$. Further comparisons of average observed deposition with model average deposition along the downline distances are provided in Section 4.2.

Figure 4-3 shows calculated and observed deposition at ground level beneath the slash pine canopy for Trial 2. The averaging techniques are the same as those used to obtain the results shown in Figure 4-1 for observed deposition and were applied to rows G-1, G-3, G-4 and G-6. Figure 4-3 shows that the peak-to-trough ratios of the model calculations, also made using σ_0 based on Equation (3-3), are smaller than the corresponding ratios for the top of the canopy shown in Figure 4-1 but larger than the ratios indicated by the observed deposition. Also, the average model deposition along the downline distance is in better agreement with the observed average ground-level deposition than for the top of the canopy.

After Trial 2, the Stearman flew at an altitude of only 5 feet (1.5 meters) above the canopy. The Hughes helicopter flew at an altitude of 5 feet (1.5 meters) above the canopy on all trials. Consequently, Equation (3-3) yields smaller values of σ_0 than for Trial 2. Figure 4-4 shows observed and calculated deposition patterns at the top of the canopy for Trial 3. Trial 3 was conducted with the Stearman under meteorological conditions similar to Trial 2, except that vertical turbulence (indicated by σ_E in Table 3-2) was greater. The use of larger values of σ_E in the model calculations would, if atmospheric dispersion dominated the deposition process at the top of the canopy, act to decrease the peak-to-trough ratios in the model-calculated deposition pattern. However, Figure 4-4 shows that the calculated deposition pattern still exhibits much greater peak-to-trough ratios than the observed pattern, indicating that the value assigned to σ_0 is the dominant factor. The figures in Appendix C for deposition at the canopy top for the helicopter trials (Trials 10, 11 and 13) also show that we have underestimated the value of σ_0 in the model calculations. The peak-to-trough ratios for the model patterns for Trials 6 and 7 in Appendix C agree better with the observed ratios, possibly because the mean wind speeds for these trials were greater.

The value of the initial source dimension σ_0 is principally controlled by the aircraft wake effects. The wake effects of the relatively slow flying helicopter (air speeds of 11 to 14 m s^{-1}) are much greater than those for the Stearman. We believe the discrepancy between the peak-to-trough ratios of the observed and calculated patterns is due to our inability to define σ_0 as a function of the fixed-wing and

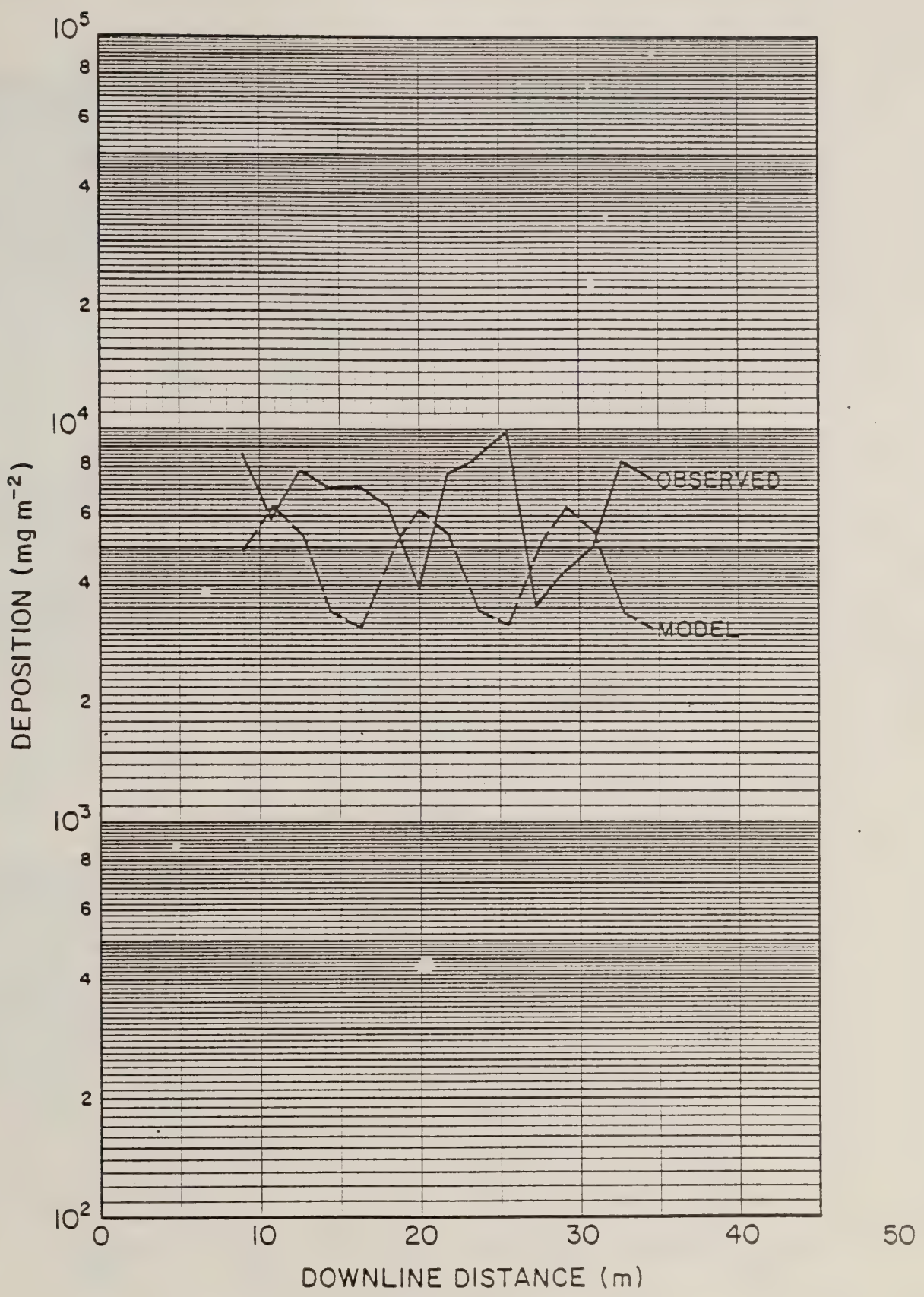


FIGURE 4-2. Observed and model deposition at the top of slash pine canopy for Trial 2, Withlacoochee Spray Trials, Florida, 1980, using an initial source dimension σ_0 twice as large as that used in the model calculations shown in Figure 4-1.

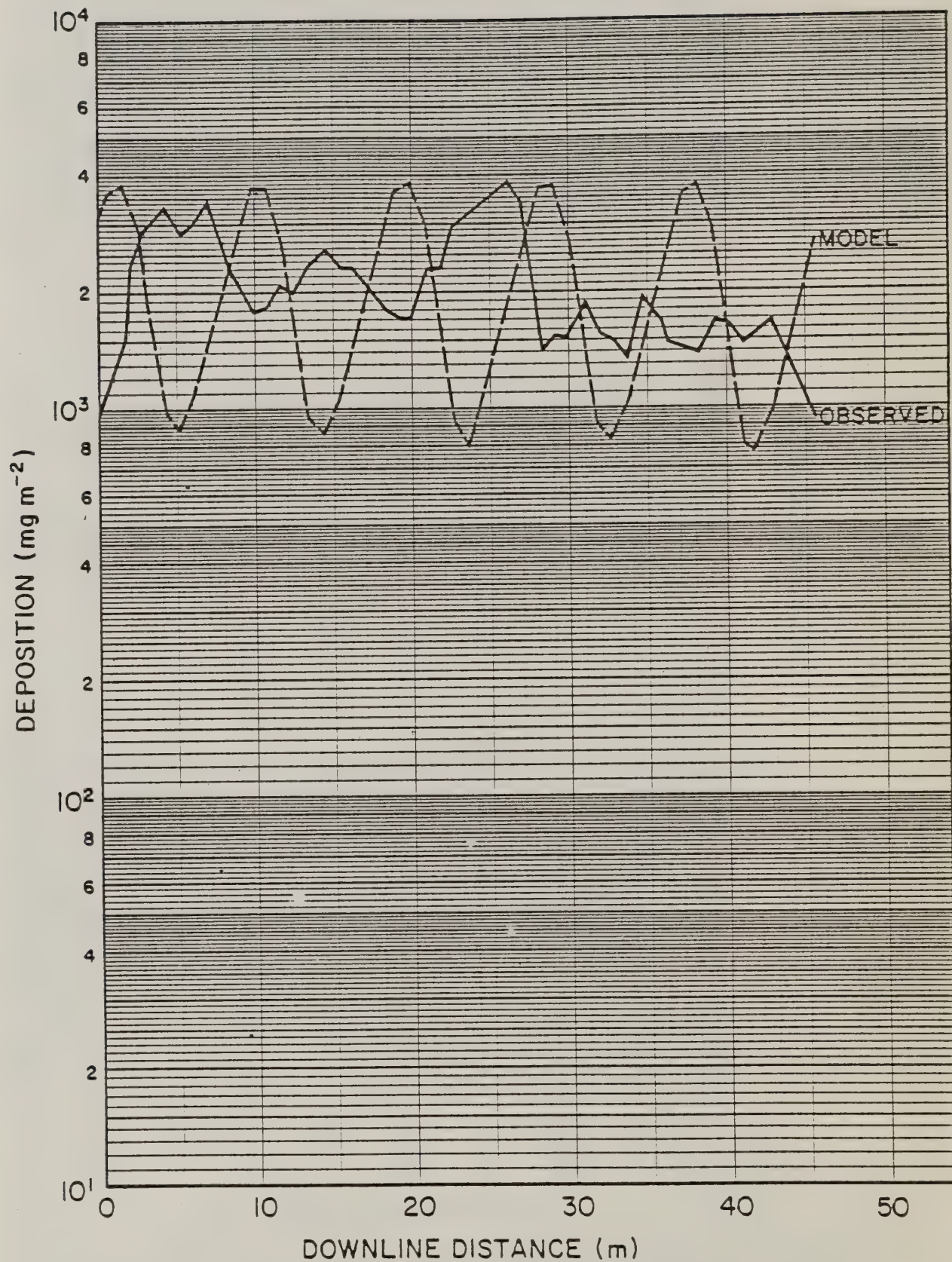


FIGURE 4-3. Observed and model ground-level depositions below the slash pine canopy for Trial 2, Withlacoochee Spray Trials, Florida, 1980.

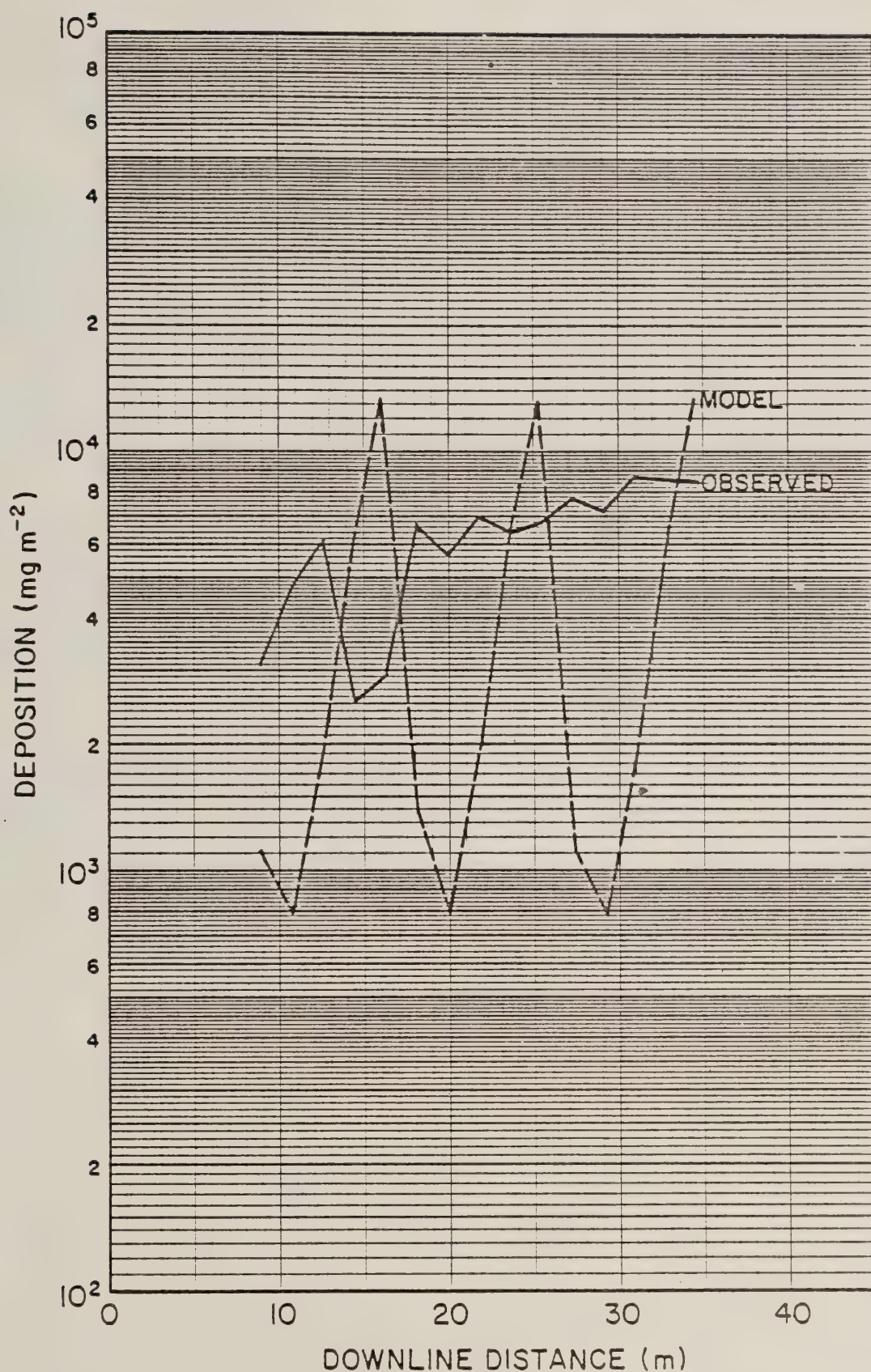


FIGURE 4-4. Observed and model deposition at the top of the slash pine canopy for Trial 3, Withlacoochee Spray Trials, Florida, 1980.

helicopter wake effects for these low-level flights. The value of σ_0 used in the model calculations also affects the average deposition levels along the downline distances, but to a lesser degree.

4.2 Ratios of Model to Observed Average Deposition Levels

A measure of the overall model performance in calculating deposition at the top of the slash and Ocala pine canopies, and at ground level beneath the trees, is obtained by forming the ratio of model to observed average deposition along the sampling lines. Both the model and observed average deposition levels were obtained by summing deposition levels over all samplers and dividing by the total number of samplers. The results are presented in Table 4-1. The value of 0.80 shown for the ratio at the slash pine canopy top for Trial 2 is the ratio of the model average deposition level along the downline distance ($5.776 \times 10^3 \text{ mg m}^{-2}$) to the observed deposition level ($7.219 \times 10^3 \text{ mg m}^{-2}$) shown in Figure 4-1.

Table 4-1 shows the observed average deposition levels are greater than model deposition levels at the slash pine canopy top on all trials and at the Ocala sand pine canopy top on all trials except Trials 1 and 2. Thus, there appears to be a bias in the model towards underprediction of the deposition at the canopy top. We believe that this is caused by the failure of the model to account for aircraft wake effects. Also, the ratios for trials conducted under similar conditions fluctuate over a large range. For example, the ratio in Table 4-1 for Trial 5 at the top of slash pine canopy is 0.25 and for Trial 6, conducted under nearly identical conditions, the ratio is 0.75. We have compared the average observed deposition with the average deposition that should have occurred if all the material released by the aircraft deposited uniformly within the spray grid area, assuming no spray drift took place. The results are shown in Table 4-2, where the average mean deposition for total recovery TR is calculated from the expression

$$TR \text{ (mg m}^{-2}\text{)} = \frac{1000 Q}{SW} \quad (4-1)$$

where

Q = source strength in g m^{-1} (see Table 3-4)

SW = swath width or distance between tree rows for these trials (9.1 m)

The ratios of observed deposition levels to the calculated levels based on total recovery clearly show that, for most trials, the observed deposition levels obtained from the Kromekote card samplers indicate more material was deposited than appears reasonable. Difficulties in the analysis of the Kromekote card data were reported by FMP/MAG due to heavy drop density on the cards and, in some cases, spreading of drop stains because the cards were dampened by dew or mist. Under these

TABLE 4-1
RATIOS OF MODEL TO OBSERVED AVERAGE DEPOSITION ALONG THE
DOWNWIND SAMPLING LINES*

Trial Number	Slash Pine Canopy		Ocala Sand Pine	
	Top	Ground	Top	Ground
2	0.80	1.03	1.11	0.42
3	0.75	1.18	1.40	0.96
5	0.25	0.86	0.30	0.18
6	0.75	0.67	**	0.17
7	0.25	0.32	0.43	0.05
10	0.20	0.80	0.25	0.52
11	0.26	0.56	0.26	0.50
13	0.50	1.11	0.50	0.61
Geometric Mean Ratio	0.41	0.76	0.49	0.32

* Based on mass deposition

** No measured data

TABLE 4-2
AVERAGE OBSERVED DEPOSITION AND AVERAGE DEPOSITION BASED ON
TOTAL RECOVERY AT THE CANOPY TOP

Trial Number	Average Observed Deposition (mg m ⁻²)		Total Recovery, TR (mg m ⁻²)	Ratio Observed/Total Recovery	
	Slash Pine	Ocala Sand Pine		Slash Pine	Ocala Sand Pine
2	7.219×10^3	5.029×10^3	6.270×10^3	1.15	0.80
3	6.412×10^3	3.432×10^3	5.280×10^3	1.21	0.65
5	1.431×10^4	1.490×10^4	5.059×10^3	2.83	2.95
6	3.234×10^3	*	3.961×10^3	0.82	*
7	2.136×10^3	1.229×10^3	9.142×10^2	2.34	1.34
10	2.623×10^4	2.386×10^4	5.047×10^3	3.19	2.75
11	2.828×10^4	1.522×10^4	6.096×10^3	2.98	2.50
13	9.184×10^3	7.296×10^3	6.096×10^3	1.51	1.20

* No samplers were placed in the Ocala sand pine canopy on this trial.

circumstances, the Quantimet Image Analyzer may have made inaccurate measurements in counting and sizing drop stains, due to the high drop densities, that lead to both overestimation of mass deposition and variability in the ratios.

Since it is unrealistic to expect the model to predict deposition levels at the canopy top greater than those based on total recovery, we have constructed adjusted ratios of model average deposition levels to "observed" deposition levels. The adjusted ratios were obtained using the deposition levels based on total recovery given in Table 4-2 as observed deposition levels when the ratios in Table 4-2 indicated more material was deposited than appears reasonable (ratios greater than unity in Table 4-2). The results of adjusting the ratios are shown in Table 4-3. We believe the ratios given in Table 4-3 more accurately reflect model performance in predicting average deposition levels. Furthermore, we would expect the observed average deposition levels at the top of the canopy to be less than those based on total recovery. If the observed deposition levels were less than those based on total recovery, the geometric mean ratios in Table 4-3 would be increased.

Drop densities on the cards beneath trees on the ground sampling rows were generally less than those at the top of the canopy, although between rows there were some very high drop densities and moisture on the cards was a problem in some trials. If the counting and sizing of drops on these cards were more accurate and the canopy penetration model performs well, we would expect the ratios for the ground sampling rows in Table 4-1 to compare favorably with the adjusted ratios in Table 4-3 for the top of the canopy. Comparison of these ratios in the two tables indicates that the ratios for the slash pine (0.76 and 0.75, respectively) are comparable. However, the geometric mean value for the ground sampling rows beneath the Ocala sand pine (0.32) is much less than the geometric mean ratio for the Ocala sand pine canopy (0.80) in Table 4-3. This may indicate, for example, that the value assigned to the probability of penetration ($PRPEN = 0.13$) for the Ocala sand pine canopy was too small while the value assigned to the slash pine canopy ($PRPEN = 0.38$) was more realistic. However, the large trial-to-trial variation of the ratios in Table 4-1 for the ground sampling rows beneath the Ocala sand pine canopy most likely indicate that other factors are involved.

As noted in previous sections, Mylar samplers were used on Trials 5, 7 and 10 and an atomic absorption technique used to analyze for manganese salts in the washed samples. Deposition estimates based on these measurements were available for six locations along each ground and canopy-top sampling line for these trials. The canopy-top samplers (soft drink cans) had Mylar on the top of the can as well as around the sides of the can. The Mylar from the top and sides of the can was washed and analyzed simultaneously. Since the deposition model calculations are only strictly comparable with deposition measurements from the top of the can, comparison with the observed deposition measurements based on this analysis is not possible. The ground Mylar samplers were placed in Kromekote card holders and the results of the atomic absorption

TABLE 4-3
ADJUSTED RATIOS OF MODEL TO OBSERVED AVERAGE DEPOSITION
LEVELS AT THE CANOPY TOP

Trial Number	Slash Pine Canopy	Ocala Sand Pine Canopy
2	0.92	1.11
3	0.91	1.40
5	0.70	0.89
6	0.75	*
7	0.59	0.58
10	0.65	0.69
11	0.77	0.65
13	0.76	0.60
Geometric Mean Ratio	0.75	0.80

* No samplers were placed in the Ocala sand pine canopy on this trial.

analysis can be directly compared with the results from the ASCAS analysis of the Kromekote cards and with the model calculations. Table 4-4 shows average observed deposition values obtained by arithmetically averaging the deposition values available from all Kromekote cards and Mylar samplers beneath the slash and Ocala sand pine canopies. The Mylar samplers were placed next to the Kromekote card samplers at positions 30 through 35 along the sampling lines (approximately in the center of the sampling line in the vicinity of the sampling trees) and spanned a distance of 4.6 meters along the sampling line. The average observed values for the Mylar and Kromekote samplers beneath the slash pine canopy agree reasonably well for Trials 5 and 7 and beneath the Ocala sand pine canopy for only Trial 7. There is very poor agreement between the two measurement techniques on Trial 10. In fact, the Mylar samplers show average deposition levels greater than expected from total recovery (5047 mg m^{-2}). Since the Mylar samples spanned a relatively short distance along the sampling line, spatial positioning of the model-calculated peaks and troughs with respect to the line and the peak-to-trough ratios of the model pattern can greatly affect the model comparison with the measurements. For example, in Trial 10 for the slash pine canopy, the model pattern has sharp peaks and troughs because of a failure adequately to account for the wake effects of the helicopter. As a result, the model shows the Mylar samplers to be closer to a trough in the calculated pattern while the measurements indicate that they are closer to a peak in the pattern. Therefore, the model greatly under-predicts the observed calculations indicated by either of the measurement techniques. For the samplers beneath the slash pine canopy on Trials 5 and 7 where the two measurement techniques agree and the model pattern does not show extreme ranges in deposition between the peaks and troughs, the model calculations and the measurements are in closer agreement.

The results of the calculations described above are summarized in Section 5.

TABLE 4-4
 AVERAGE OBSERVED (MYLAR AND KROMEKOTE SAMPLERS)
 AND MODEL DEPOSITION LEVELS (mg m⁻²) FOR
 GROUND SAMPLERS BENEATH THE CANOPY*

Trial Number	Canopy	Average Observed (Mylar Sampler)	Average Observed (Kromekote Sampler)	Model Average
5	Slash	1096	986	928
	Ocala	417	278	140
7	Slash	373	396	266
	Ocala	113	149	10
10	Slash	8425	2762	80
	Ocala	5454	1020	755

* The values given in the Table for Kromekote samplers and the model calculations are based on deposition values for the positions where both Mylar and Kromekote samplers were located.

SECTION 5 SUMMARY AND RECOMMENDATIONS

5.1 Summary of Results

The CBG model computer program has been used to calculate deposition patterns for comparison with measurements made at the canopy top and on the ground beneath the canopy in the Withlacoochee spray trials. The deposition patterns at the canopy top discussed in Section 4.1 show that the peaks and troughs of model deposition patterns for the fixed-wing aircraft are exaggerated compared to the measured patterns, especially under low wind-speed conditions. The model peaks and troughs for the helicopter deposition patterns are also greatly exaggerated compared to the observed patterns. At ground level, the model deposition patterns for the fixed-wing aircraft more nearly approximate the observed deposition patterns, while the model helicopter patterns do not. We believe the failure of the model calculations to match the shape of the observed patterns is caused by aircraft wake effects that are not adequately accounted for in the model. In almost all the Withlacoochee trials, both aircraft flew at a height of about 1.5 meters above the canopy. The wake effects expressions in the CBG model assume that the minimum aircraft altitude above the top of the canopy is greater than one-half the wing span (11.48/2 meters) or rotor diameter (8.03/2 meters). In all previous tests of the performance of the CBG model in calculating deposition patterns from fixed-wing spray aircraft and helicopters (Dumbauld, Rafferty and Cramer, 1976; Dumbauld, Rafferty and Bjorklund, 1977) the above-canopy flight altitudes were larger than the minimum altitude assumed in the wake effects expressions and the shapes of the model and observed deposition patterns were similar.

Table 5-1 shows geometric mean ratios of model to observed average mass deposition at the canopy top of the slash and Ocala sand pines and at the ground beneath the canopies. According to these ratios, the CBG model program underestimates the deposition at the top of the slash pine canopy by more than a factor of 2, and underestimates the deposition at the ground by a factor of 1.3. The model also underestimates the average deposition at the canopy top of the Ocala sand pine by a factor of 2 and at the ground by a factor of 3. However, the observed average depositions reflected in these ratios are larger than expected if all the material emitted by the spray aircraft entered the canopy. We believe this anomalous result is explained in part by limitations of the Quantimet drop counting and sizing analysis. High density of drops on the sampling cards and the presence of moisture on the cards during some trials resulted in an overestimation of the mass deposition on the cards. This was due to inability of the Quantimet to distinguish single drops from drops which touch. Also, dampness causes excessive spreading on Krome kote cards and thus an overestimate of drop size and spray volume. For these reasons, we adjusted the average deposition levels at the canopy top so that they did not exceed the values expected from total recovery based on the application rate Q (see Table 3-4). Table 5-2 shows adjusted geometric

TABLE 5-1
GEOMETRIC MEAN RATIOS OF AVERAGE MODEL TO OBSERVED
MASS DEPOSITION FOR THE WITHLACOOCHEE SPRAY TRIALS

Tree Type	Canopy Top			Ground		
	Fixed Wing	Helicopter	Combined	Fixed Wing	Helicopter	Combined
Slash Pine	0.49	0.30	0.41	0.74	0.79	0.76
Ocala Sand Pine	0.67	0.32	0.49	0.23	0.54	0.32

TABLE 5-2
ADJUSTED* GEOMETRIC MEAN RATIOS OF MODEL TO
OBSERVED MASS DEPOSITION AT THE CANOPY TOP

Tree Type	Fixed Wing	Helicopter	Combined
Slash Pine	0.76	0.72	0.75
Ocala Sand Pine	0.95	0.65	0.80
Combined	0.84	0.68	0.77

* Adjusted to account for possible errors in counting and sizing drops

mean ratios of model to observed average mass deposition using the adjusted levels. The model calculations underestimate the observed average deposition at the canopy top by about a factor of 1.3 after this adjustment was made.

Since the adjusted geometric mean ratio for the slash pine canopy top in Table 5-2 (0.75) agrees with the ratio for ground level beneath the canopy in Table 5-1, it appears that model inputs to the canopy penetration model (Grim and Barry, 1975) in the CBG computer program have been chosen correctly. On the other hand, the difference of the ratios for the Ocala sand pine at the top of the canopy and at the ground indicates that the inputs to the model for Ocala sand pine require further adjustment.

Manganese salts were added to the spray material during 3 trials as a chemical tracer to permit a subsequent direct analysis of mass deposition using atomic absorption techniques. Comparison of observed average deposition at the canopy top and beneath the canopy based on this analysis technique with the average deposition obtained from the drop counting and sizing technique show poor agreement between the two analysis methods. Only a limited number of the Mylar samplers were used to collect spray deposition for the atomic absorption analysis and this technique was used only in 3 trials. For this reason there were insufficient deposition data based on this analysis technique for adequate assessment of the model performance.

In spite of the expected difficulties in applying the CBG model for use with low-flying aircraft, we believe the results of this study demonstrate the feasibility of adapting the CBG model for applications in planning and conducting aerial application programs in seed orchards.

5.2 Recommendations

As explained above, serious problems were encountered in adequately accounting for the wake effects of low-flying aircraft and in the counting and sizing of drops under the experimental constraints of the Withlacoochee Spray Trials. The results clearly show that improvement in the wake model, used to obtain source dimensions, is required to adequately describe the shapes of deposition patterns when the aircraft flight altitude is in close proximity to the top of the canopy. Until this improvement is made, the utility of the model in defining optimum spray aircraft altitudes and swath widths for orchard spray operations is limited. The estimation of spray drift, specification of buffer zones, and effective deposition levels within the canopy depends in part on the ability to calculate accurately the deposition at the top of the canopy. To properly assess the utility of the CBG model computer program in calculating average deposition requires more quantitative deposition measurements than those made during the Withlacoochee trials.

Because of funding and time limitations, we have been unable to utilize all the data available from the Withlacoochee trials to improve model performance. For example, larger values for the model input

PRPEN describing the probability of a drop penetrating a tree may result in more accurate estimates of ground-level deposition and canopy retention of drops for trees similar to the Ocala sand pine, which had denser foliage than the slash pine.

We make the following recommendations for future work:

- Efforts should be made to improve the wake model portion of the CBG program concept for low-flying aircraft
- The manganese salt tracer technique should be further assessed as a means of measuring mass deposition in cases where Kromekote cards are expected to show high drop densities
- Further analysis of the Withlacoochee trial data should be performed to improve model parameteric inputs and reassess model performance where practical

Acknowledgements

The authors wish to thank Ms. Patricia Kenney, FPM/MAG, for editing the deposition and other data obtained during the Withlacoochee Spray Trials. We sincerely appreciate the assistance provided by Mr. Larry Barber, SA-FPM and Mr. Robert Eckblad, MEDC, Montana, in preparation for and conduct of the spray trials. Mr. Hoover Lambert and Mr. Thomas Gentry, SA-FPM, assisted us in installing meteorological equipment prior to the trials and in the maintenance of the equipment during the trials. Mr. Lacy Hancock, H. E. Cramer Company, operated the meteorological equipment during the trials and reduced the meteorological data for use in this study. Finally, we thank Mr. Robert Carr, NASA, Wallops Flight Center, for providing us with the Vectorvanes and towers used to make the meteorological measurements and U. S. Army Dugway Proving Ground for providing the wind recorders.

LITERATURE CITED

Dumbauld, R. K., H. E. Cramer and J. W. Barry, 1975: Application of meteorological prediction models to forest spray problems. Paper presented at the USDA Forest Service Workshop, Aerial Application of Insecticides Against Forest Defoliators, Missoula, Montana, April 1974. DPG Document No. DPG-TR-M935P, U. S. Army Dugway Proving Ground, Dugway, Utah 84022.

Dumbauld, R. K., J. E. Rafferty and H. E. Cramer, 1976: Dispersion deposition from aerial spray releases. Paper presented at the Third Symposium on Atmospheric Turbulence, Diffusion and Air Quality Raleigh, North Carolina. Reprint available from American Meteorological Society, Boston, Massachusetts.

Dumbauld, R. K. and J. R. Bjorklund, 1977: Deposition profile calculations for the State of Maine 1977 spray program. H. E. Cramer Company, Inc. Technical Report TR-77-310-01 prepared for Litton Aero Products, Woodland Hills, California and the State of Maine Bureau of Forestry, Augusta, Maine.

Dumbauld, R. K., J. E. Rafferty and J. R. Bjorklund, 1977: Prediction of spray behavior above and within a forest canopy. Special Report Under Contract No. 19-276, Pacific N. W. Forest and Range Experiment Station, Portland, Oregon. Published by Methods Application Group, USDA Forest Service, Davis, California.

Fritsch, L. J., et al., 1970: Dispersion of air tracers into and within a forested area: 3. Report No. TR ECOM-68-G8-3, Atmospheric Sciences Laboratory, Ft. Huachuca, Arizona.

GCA Corporation, 1971: Model estimates of the deposition of aerial spray on a forest canopy. Technical Note, contract No. DAAD09-71-C-0003 with U. S. Army Dugway Proving Ground, Dugway, Utah 84022.

Grim, B. S. and J. W. Barry, 1975: A canopy penetration model for aerially disseminated insecticide spray released above coniferous forests. Final Report under MEDC Project No. 2425, Forest Service Equipment Development Center, Missoula, Montana.

H. E. Cramer Company, 1973: Model estimates of deposition and concentration for the 1973 field tests of insecticides on Pine Butterfly Larval population in the Bitterroot National Forest. Technical Note prepared under Contract No. DAAD09-71-C-0003 with U. S. Army Dugway Proving Ground, Dugway, Utah 84022.

McDonald, J. E., 1960: An aid to computation of terminal fall velocities of spheres. J. Met., 17, 463.

Rafferty, J. E. and R. K. Dumbauld, 1980: Selection of spray operations criteria for the Withlacoochee State Orchard project. Report No. 80-8 under Contract No. 53-01S8-9-6260, Methods Application Group, USDA Forest Service, Davis, California.

APPENDIX A
DESCRIPTION OF THE CBG DEPOSITION AND
CANOPY PENETRATION MODELS

A.1 CBG Deposition Model

In the model, the axis of the spray cloud is assumed to intersect the ground at a downwind distance from the source that is proportional to the product of the release height H and the mean cloud transport speed \bar{u} divided by the drop settling velocity V_j for the j th drop-size category. The inclination of the cloud axis from the horizontal for a given drop-size category j is thus equal to $\tan^{-1}(V_j/\bar{u})$. It is assumed that drops dispersed upwards by turbulence are totally reflected downwards at the top of the surface mixing layer, but the fraction of drops reflected at the ground is a variable input parameter for each j th category. The model uses the Cartesian coordinate system shown in Figure A-1 for a line source of length L at a height H and a calculation point at $R(\epsilon, \delta, z)$. Deposition, expressed in units of mass per unit area, at the point $(\epsilon, \delta, 0)$ is given by the expression

$$\text{Dep}_L = \frac{2S}{\sin\theta} \sum_{j=1}^J f_j (1 - \gamma_j) \left\{ \frac{B \exp\left(\frac{G^2}{4F} - P\right)}{2F} \left[\exp\left[-\left(F^{1/2} \left(\frac{1}{a} - \frac{G}{2F}\right)\right)^2\right] \right. \right. \quad (A-1)$$

$$\left. \left. - \left[\exp\left[-\left(F^{1/2} \left(\frac{1}{b} - \frac{G}{2F}\right)\right)^2\right] \right] + \frac{G B \pi^{1/2} \exp\left(\frac{G^2}{4F} - P\right)}{4F^{3/2}} \right\}$$

$$\left[\text{erf}\left(F^{1/2} \left(\frac{1}{b} - \frac{G}{2F}\right)\right) - \text{erf}\left(F^{1/2} \left(\frac{1}{a} - \frac{G}{2F}\right)\right) \right]$$

$$+ \sum_{i=1}^{\infty} \left\{ \gamma_{j-i} \frac{C \exp\left(\frac{J^2}{4I} - P\right)}{2I} \left[\exp\left[-\left(I^{1/2} \left(\frac{1}{a} - \frac{J}{2I}\right)\right)^2\right] \right. \right.$$

$$\left. \left. - \exp\left[-\left(I^{1/2} \left(\frac{1}{b} - \frac{J}{2I}\right)\right)^2\right] \right] + \frac{J C \pi^{1/2} \exp\left(\frac{J^2}{4I} - P\right)}{4I^{3/2}} \right\}$$

(Equation (A-1) continued on following page.)

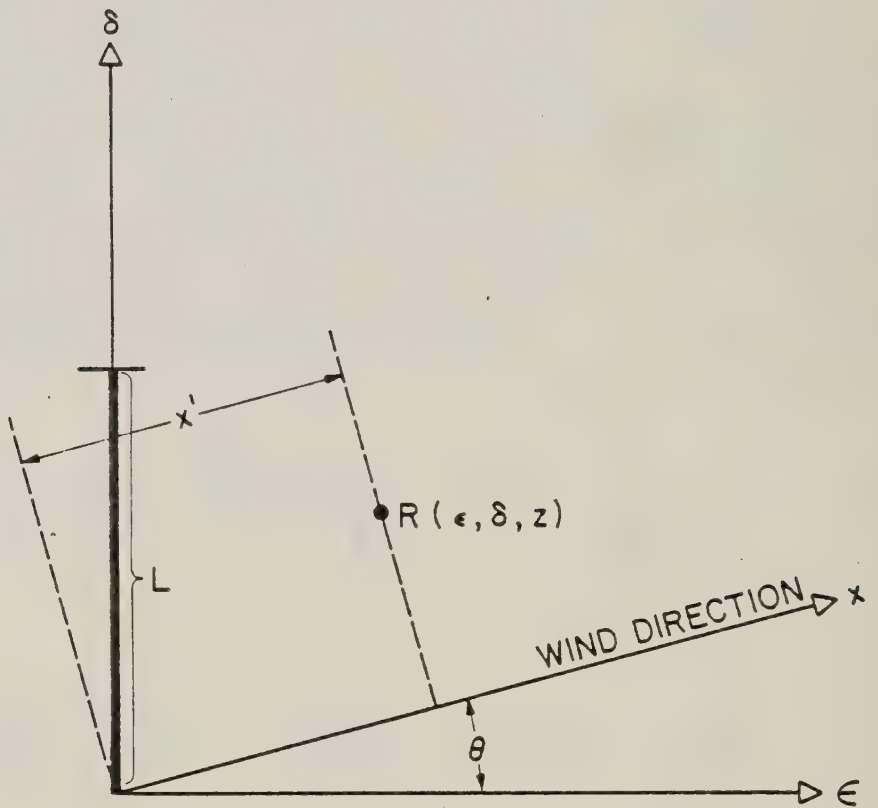


FIGURE A-1. Schematic diagram showing the line source geometry with respect to a calculation point at $R(\epsilon, \delta, z)$ and wind direction θ .

(Equation (A-1) Continued.)

$$\begin{aligned}
 & \left[\operatorname{erf} \left(I^{1/2} \left(\frac{1}{b} - \frac{J}{2I} \right) \right) - \operatorname{erf} \left(I^{1/2} \left(\frac{1}{a} - \frac{J}{2I} \right) \right) \right] \\
 & + \gamma_j \frac{D \exp \left(\frac{K^2}{4E} - P \right)}{2E} \left[\exp \left[- \left(E^{1/2} \left(\frac{1}{a} - \frac{K}{2E} \right) \right)^2 \right] - \exp \left[- \left(E^{1/2} \left(\frac{1}{b} - \frac{K}{2E} \right) \right)^2 \right] \right] \\
 & + \gamma_i \frac{KD\pi^{1/2} \exp \left(\frac{K^2}{4E} - P \right)}{4E^{3/2}} \left[\operatorname{erf} \left(E^{1/2} \left(\frac{1}{b} - \frac{K}{2E} \right) \right) - \operatorname{erf} \left(E^{1/2} \left(\frac{1}{a} - \frac{K}{2E} \right) \right) \right] \} \}
 \end{aligned} \tag{A-1}$$

where

$$S = Qk/2\pi \tag{A-2}$$

$$B = H' + \frac{V_j x_v}{D} \tag{A-3}$$

$$G = \frac{2^{1/2}}{\sigma'_A} \left[\frac{V_j B k^2}{\bar{u}} + \left(n - \frac{\delta}{\cos \theta} \right) \cot \theta \right] \tag{A-4}$$

$$F = k^2 B^2 + \left(n - \frac{\delta}{\cos \theta} \right)^2 \tag{A-5}$$

$$J = \frac{-2^{1/2}}{A} \left[\frac{V_j C k^2}{\bar{u}} + \left(n - \frac{\delta}{\cos \theta} \right) \cot \theta \right] \tag{A-6}$$

$$I = k^2 C^2 + \left(n - \frac{\delta}{\cos \theta} \right)^2 \tag{A-7}$$

$$P = \left[\frac{KV_j}{2^{1/2} \sigma'_A \bar{u}} \right]^2 + \left[\frac{\cot \theta}{2^{1/2} \sigma'_A} \right]^2 \tag{A-8}$$

$$K = \frac{2^{1/2}}{\sigma_A'} \left[\frac{v_j D k^2}{\bar{u}} + \left(n - \frac{\delta}{\cos \theta} \right) \cot \theta \right] \quad (A-9)$$

$$E = k^2 D^2 + \left(n - \frac{\delta}{\cos \theta} \right)^2 \quad (A-10)$$

$$C = 2iH_m - H - \left(v_j x_v / \bar{u} \right) \quad (A-11)$$

$$D = 2iH_m + H + \left(v_j x_v / \bar{u} \right) \quad (A-12)$$

$$a = 2^{1/2} \sigma_A' (x' + x_v) \quad (A-13)$$

$$b = 2^{1/2} \sigma_A' (x' + x_v - \ell \sin \theta) \quad (A-14)$$

$$n = (x' + x_v) \cot \theta + x' \tan \theta = (\varepsilon / \sin \theta) + (\delta / \cos \theta) + x_v \cot \theta \quad (A-15)$$

$$x' = (\varepsilon + \delta \tan \theta) \cos \theta = \varepsilon \cos \theta + \delta \sin \theta \quad (A-16)$$

x_v = virtual distance

$$= \frac{k \sigma_0}{\sigma_A'} - x_R \quad (A-17)$$

ℓ = effective line length

$$= \begin{cases} \delta + \varepsilon \cot\theta ; \quad \delta + \varepsilon \cot\theta \leq L \\ L \quad ; \quad \delta + \varepsilon \cot\theta > L \end{cases} \quad (A-18)$$

The following parameters used in the preceding equations are based on meteorological measurements or inferred from meteorological measurements:

σ'_A = standard deviation of the wind azimuth angle in radians

k = constant relating σ'_A and σ'_E

$$= \sigma'_A / \sigma'_E \quad (A-19)$$

σ'_E = standard deviation of the wind elevation angle in radians

H_m = depth of the surface mixing layer below a capping inversion

\bar{u} = mean transport wind speed

$$= \begin{cases} \frac{\bar{u}_R [z_2^{1+p} - z_1^{1+p}]}{(z_2 - z_1)(z_R)^p (1+p)} ; \quad \bar{u} > \bar{u}_R \\ \bar{u}_R \quad ; \quad \bar{u} \leq \bar{u}_R \end{cases} \quad (A-20)$$

\bar{u}_R = mean wind at the reference height z_R

p = wind power-law coefficient

z_2 = effective upper bound of the cloud

$$= \begin{cases} H + 2.15 \left(\frac{kx'}{\sigma_A} + x_V \right) & ; \quad z_2 < H_m \\ H_m & ; \quad z_2 \geq H_m \end{cases} \quad (A-21)$$

z_1 = effective lower bound of the cloud

$$= \begin{cases} H' - 2.15 \left(\frac{kx'}{\sigma_A} + x_V \right) & ; \quad z_1 > 2 \\ 2 & ; \quad z_1 \leq 2 \end{cases} \quad (A-22)$$

θ = angle between a line perpendicular to the line source and the mean wind direction (see Figure A-1)

The following parameters are source inputs required for use in the model:

Q = total source strength emitted along the length L of the line source

H = release height

v_j = gravitational settling velocity for the median drop by mass in the j^{th} drop-size category

f_j = fraction of the total source strength in the j^{th} drop-size category

γ_j = reflection coefficient for the median drop by mass in the j th drop-size category

σ_0 = standard deviation of the cloud distribution at the distance x_R

x_R = distance from the line source to cloud stabilization

L = length of the line source

Despite the apparent complexity of the model, solution times are relatively short because the summation for multiple reflection from $i=0$ to infinity usually can be terminated after less than 10 passes (by checking to see if succeeding passes result in significant increases in the calculated deposition). Also, as shown by the model equations, the solution fails when the wind is exactly perpendicular to the line source ($\theta=0$ degrees) or when the wind direction is exactly parallel to the line source ($\theta=90$ degrees). Exact solutions for these angles are easily derived. However, it is simpler to have the computer program change these angles by a small fraction (0.01 degrees) and then calculate the deposition because there is no significant loss in accuracy.

A.2 CBG Canopy Penetration Model

The model is based on a Monte Carlo technique where a large number of drops in each size category are passed along a trajectory through a simulated forest with trees assigned to equal areas according to the density (stems per acre) in the forest being simulated. The drop trajectory is a function of the gravitational settling velocity V_j and the mean wind speed at various levels within the forest canopy. As a drop proceeds along the trajectory, each tree is randomly displaced within the assigned area in the plane of the horizon and calculations are made to determine if the drop intersects the tree envelope and, if an intersection occurs, whether the drop strikes a tree element. When the drop strikes a tree element, a tally is recorded for the height interval within the canopy where the "hit" occurs and for all greater height intervals. Drops proceed along the trajectory until a hit occurs or until the trajectory intersects the ground. After the specified total number of drops in the size category have passed along the trajectory, the tally number within each height interval is divided by the total number of drops to obtain the percentage of drops reaching the given height interval. The total number of drops passed along the trajectory required to achieve a stabilized solution (percentage penetration) is a function of the steepness of the trajectory, with more drops being required for size categories with large settling velocities.

Figure A-2 is a schematic diagram showing an example drop trajectory and forest construct. The drop trajectory in each of k height intervals is defined by the following piecewise linear function:

$$x_k = \begin{cases} 0 & ; k = 0 \\ \frac{0.25(k-1)H_c}{\tan \phi_k} + x_{k-1} & ; k = 1, 2, 3, 4 \end{cases} \quad (A-23)$$

$$y_k = 0 \quad (A-24)$$

$$z_k = 0.25kH_c ; k = 0, 1, 2, 3, 4 \quad (A-25)$$

where

ϕ_k = angle, measured in radians, defining the declination of the trajectory with respect to the plane of the horizon

$$= \begin{cases} \tan^{-1} \frac{v_j}{\bar{u}_{c;k}} & ; \phi \leq 1.4 \text{ radians} \\ 1.4 \text{ radians} & ; \phi > 1.4 \text{ radians} \end{cases} \quad (A-26)$$

H_c = height of the forest canopy

$\bar{u}_{c;k}$ = mean wind speed in the k^{th} height interval within the canopy

The number of trees placed along the trajectory path in the simulated forest is given by the expression

$$N_t = x_4 / \Delta x_t \quad (A-27)$$

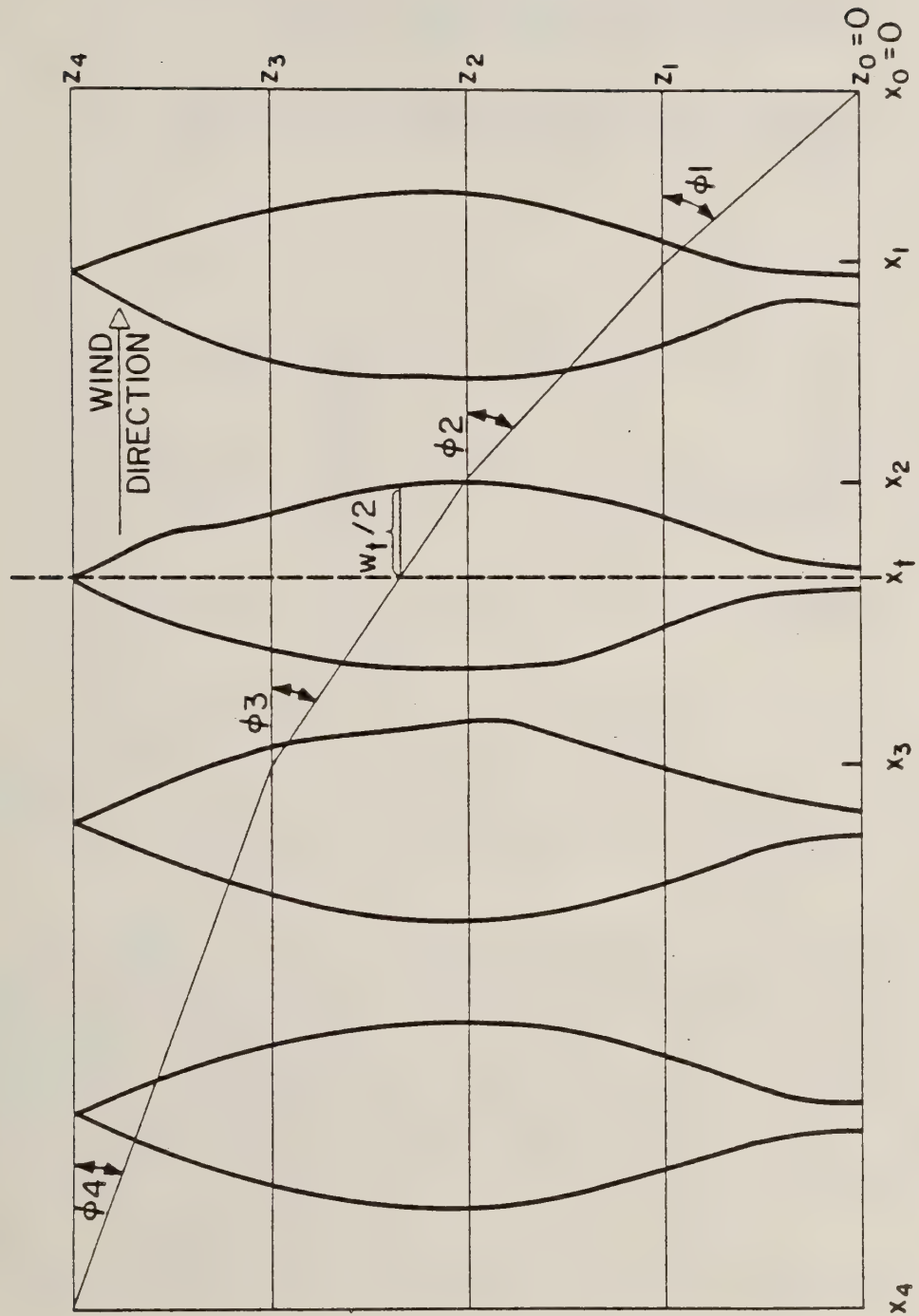


FIGURE A-2. Schematic diagram showing an example drop trajectory and simulated forest.

where

$$\begin{aligned} x_4 &= \text{maximum horizontal travel distance in meters of the drop within the forest canopy} \\ \Delta x_t &= \text{alongwind tree spacing within the simulated forest} \\ &= 63.8/\sqrt{D_t} \\ D_t &= \text{tree density in units of stems per acre} \end{aligned} \quad (A-28)$$

As shown in Figure A-2, each tree stem is given the following location along the trajectory:

$$x_t = (N_t - n) \Delta x_t + (R - 0.5) \Delta x_t ; \quad n=1,2,\dots,N_t \quad (A-29)$$

$$y_t = \left| (R' - 0.5) \Delta x_t \right| \quad (A-30)$$

where

$$n = \text{tree number}$$

and R and R' are uniform random numbers between 0 and 1. The possibility of the drop trajectory intersecting the tree envelope is determined by comparing the distance y_t with the radius of the tree envelope ($W_t/2$) at the height z_p where the trajectory passes through the distance x_t . The tree widths W_t are specified by the program user at one-meter intervals and the program calculates the radius ($W_t/2$) at z_p by linear interpolation. If y_t is greater than $(W_t/2)$, no intersection occurs and the computer program proceeds to the next tree along the trajectory.

If the drop trajectory intersects the tree envelope, the program calculates the probability that the drop impacts on a tree element from the expression

$$P_j = E_j (1 - PRPEN^{\zeta}) \quad (A-31)$$

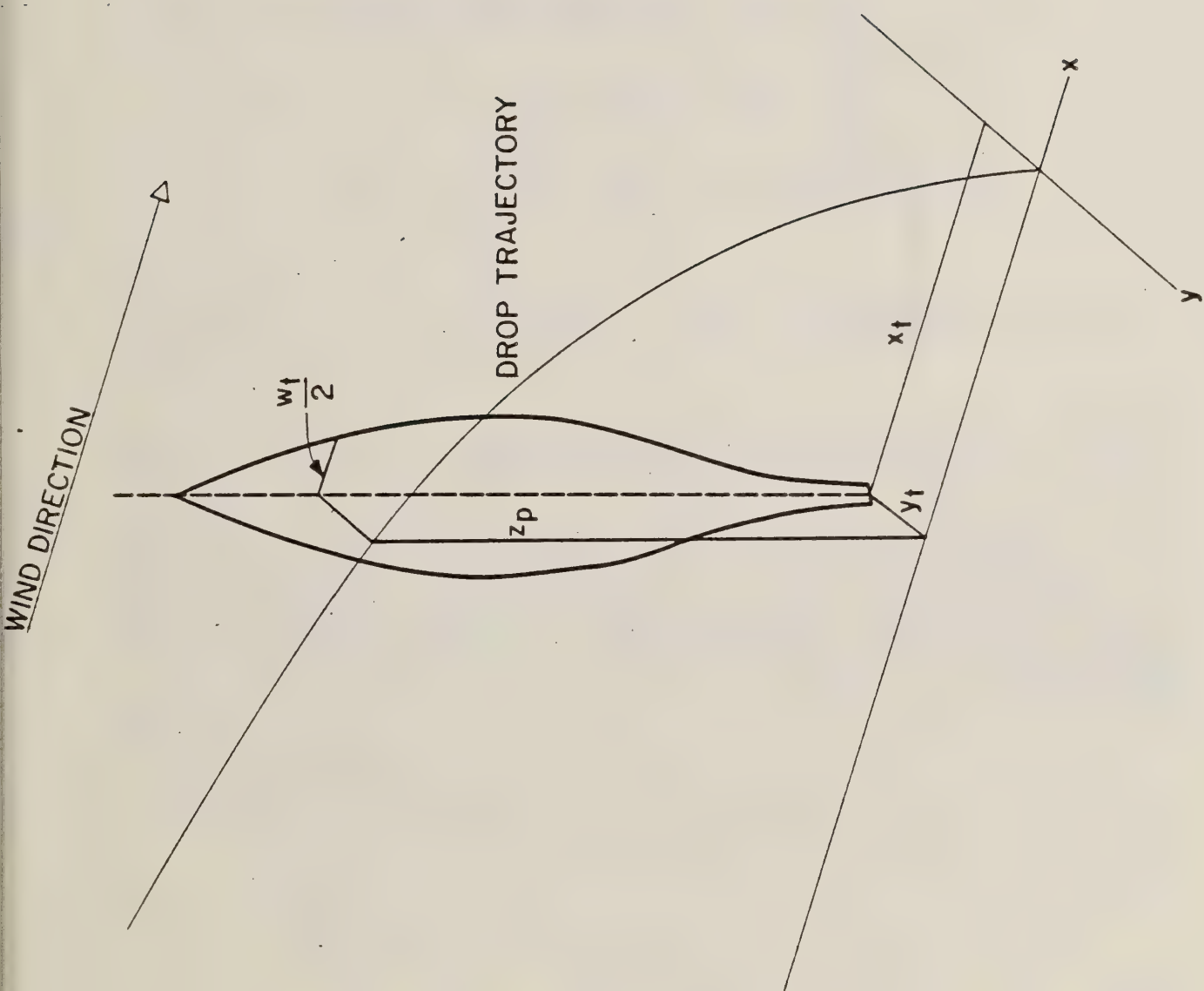


FIGURE A-3. Schematic diagram showing the coordinate location of the "random tree".

where

E_j = impaction efficiency of the tree element for the j th drop-size category

PRPEN = probability of penetration for the population of drops and for a horizontal trajectory through the tree

ζ = path length correction factor for a non-horizontal trajectory

$$\zeta = \begin{cases} \frac{1}{\cos k} & ; \quad \zeta \leq \frac{H_c}{W_m} \\ \frac{H_c}{W_m} & ; \quad \zeta > \frac{H_c}{W_m} \end{cases} \quad (A-32)$$

W_m = maximum width of the tree envelope

A particular drop of the population of drops is assumed to intersect the tree element when the value of P_j from Equation (A-31) is greater than a uniform random number R between 0 and 1. Each tree is divided into ten height-class intervals, and an intersection with a tree element is recorded as a "hit" in the class interval in which z_p occurs and in every higher class interval.

The process described above is repeated for every drop passed along the trajectory and the final percentage of material penetrating to a given height interval determined by dividing the number of recorded hits in the height interval by the total number of drops in all j th size categories passed along the trajectory.

The inputs required by the canopy-penetration model are:

PRPEN = probability of penetration

$\bar{u}_{c;k}$ = mean wind speed in the k th height interval within the forest canopy

v_j = gravitational settling velocity in meters per second for the median drop by mass in the j th drop-size category

E_j = impaction collection efficiency for the j^{th} drop-size category

D_t = tree density in stems per acre

H_c = tree height in meters

W_i = tree width at one-meter height intervals

M = total number of drops to be passed along the trajectory

The computer program also permits the user to simulate a multi-storied canopy of up to three tree heights, with a different value of PRPEN possible for each tree or story height.

The output from the canopy penetration model includes, in addition to the percentage of material in the j th drop size category penetrating to each of ten levels within the canopy, the maximum horizontal travel distance of the drop within the forest canopy (x_4). When the deposition model given by Equation (A-1) is used in conjunction with the canopy penetration model to calculate ground-level deposition within the canopy, the distance from the line source to the target is adjusted so that the deposition model calculates the deposition at the top of the forest canopy at a distance x_4 upwind from the target. The deposition at the target is then determined by multiplying the deposition predicted from Equation (A-1) by the percentage of material reaching the ground from the canopy penetration model.

APPENDIX B

This appendix contains tables of drop-size distributions and associated gravitational settling velocities, reflection coefficients and impaction efficiencies for Trials 2, 3, 5, 6, 7, 10, 11 and 13 of the Withlacoochee Spray Trials.

TABLE B-1
 DROP-SIZE DISTRIBUTION, SETTLING VELOCITIES v_j , REFLECTION
 COEFFICIENTS γ_j AND IMPACTION EFFICIENCIES E_j FOR
 TRIAL 2 OF THE WITHLACOOCHEE SPRAY TRIALS,
 FLORIDA, 1980

Drop-Size Category j	Mean Drop Diameter (μm)	f_j	v_j (m s^{-1})	γ_j	E_j
1	38.0	0.001	0.063	0.59	0.027
2	78.3	0.009	0.216	0.21	0.117
3	118	0.02	0.402	0	0.265
4	153	0.03	0.595	0	0.445
5	185	0.04	0.741	0	0.650
6	228	0.10	0.926	0	0.988
7	278	0.10	1.20	0	1
8	327	0.10	1.44	0	1
9	406	0.20	1.76	0	1
10	486	0.10	2.07	0	1
11	546	0.10	2.36	0	1
12	623	0.10	2.73	0	1
13	705	0.04	3.11	0	1
14	792	0.03	3.44	0	1
15	933	0.02	3.96	0	1
16	1231	0.01	4.93	0	1

TABLE B-2
 DROP-SIZE DISTRIBUTION, SETTLING VELOCITIES v_j , REFLECTION
 COEFFICIENTS γ_j AND IMPACTION EFFICIENCIES ϵ_j FOR
 TRIAL 3 OF THE WITHLACOOCHEE SPRAY TRIALS,
 FLORIDA, 1980

Drop-Size Category j	Mean Drop Diameter (μm)	f_j	v_j (m s^{-1})	γ_j	ϵ_j
1	44.8	0.001	0.086	0.53	0.041
2	82.8	0.009	0.230	0.17	0.141
3	121	0.02	0.414	0	0.301
4	149	0.03	0.566	0	0.456
5	175	0.04	0.699	0	0.629
6	214	0.10	0.863	0	0.940
7	257	0.10	1.08	0	1
8	293	0.10	1.27	0	1
9	353	0.20	1.54	0	1
10	415	0.10	1.79	0	1
11	463	0.10	1.98	0	1
12	525	0.10	2.25	0	1
13	592	0.04	2.57	0	1
14	661	0.03	2.91	0	1
15	728	0.02	3.20	0	1
16	792	0.01	3.44	0	1

TABLE B-3
 DROP-SIZE DISTRIBUTION, SETTLING VELOCITIES v_j , REFLECTION
 COEFFICIENTS γ_j AND IMPACTION EFFICIENCIES E_j FOR
 TRIAL 5 OF THE WITHLACOOCHEE SPRAY TRIALS
 FLORIDA, 1980

Drop-Size Category j	Mean Drop Diameter (μm)	f_j	v_j (m s^{-1})	γ_j	E_j
1	58.2	0.001	0.144	0.39	0.200
2	102	0.009	0.312	0	0.608
3	148	0.02	0.557	0	1
4	186	0.03	0.745	0	1
5	217	0.04	0.875	0	1
6	264	0.10	1.11	0	1
7	323	0.10	1.42	0	1
8	383	0.10	1.67	0	1
9	475	0.20	2.03	0	1
10	560	0.10	2.42	0	1
11	626	0.10	2.74	0	1
12	706	0.10	3.12	0	1
13	785	0.04	3.42	0	1
14	863	0.03	3.71	0	1
15	984	0.02	4.16	0	1
16	1184	0.01	4.81	0	1

TABLE B-4

DROP-SIZE DISTRIBUTION, SETTLING VELOCITIES v_j , REFLECTION COEFFICIENTS γ_j AND IMPACTION EFFICIENCIES E_j FOR TRIAL 6 OF THE WITHLACOOCHEE SPRAY TRIALS
FLORIDA, 1980

Drop-Size Category j	Mean Drop Diameter (μm)	f_j	v_j (m s^{-1})	γ_j	E_j
1	53.6	0.001	0.121	0.45	0.227
2	110	0.009	0.354	0	0.954
3	172	0.02	0.686	0	1
4	228	0.03	0.921	0	1
5	279	0.04	1.19	0	1
6	349	0.10	1.53	0	1
7	427	0.10	1.84	0	1
8	491	0.10	2.10	0	1
9	583	0.20	2.53	0	1
10	682	0.10	3.01	0	1
11	769	0.10	3.37	0	1
12	862	0.10	3.71	0	1
13	937	0.04	3.99	0	1
14	1019	0.03	4.29	0	1
15	1100	0.02	4.55	0	1
16	1217	0.01	4.92	0	1

TABLE B-5
 DROP-SIZE DISTRIBUTION, SETTLING VELOCITIES v_j , REFLECTION
 COEFFICIENTS γ_j AND IMPACTION EFFICIENCIES ϵ_j FOR
 TRIAL 7 OF THE WITHLACOOCHEE SPRAY TRIALS
 FLORIDA, 1980

Drop-Size Category j	Mean Drop Diameter (μm)	f_j	v_j (m s^{-1})	γ_j	ϵ_j
1	64.7	0.001	0.175	0.31	0.483
2	120	0.009	0.417	0	1
3	181	0.02	0.724	0	1
4	230	0.03	0.942	0	1
5	273	0.04	1.17	0	1
6	337	0.10	1.47	0	1
7	411	0.10	1.77	0	1
8	477	0.10	2.03	0	1
9	582	0.20	2.53	0	1
10	694	0.10	3.05	0	1
11	782	0.10	3.38	0	1
12	898	0.10	3.81	0	1
13	1051	0.04	4.33	0	1
14	1222	0.03	4.86	0	1
15	1335	0.02	5.21	0	1
16	1390	0.01	5.37	0	1

TABLE B-6
 DROP-SIZE DISTRIBUTION, SETTLING VELOCITIES v_j , REFLECTION
 COEFFICIENTS γ_j AND IMPACTION EFFICIENCIES ϵ_j FOR
 TRIAL 10 OF THE WITHLACOOCHEE SPRAY TRIALS
 FLORIDA, 1980

Drop-Size Category j	Mean Drop Diameter (μm)	f_j	v_j (m s^{-1})	γ_j	ϵ_j
1	59.1	0.001	0.149	0.38	0.115
2	108	0.009	0.347	0	0.385
3	161	0.02	0.635	0	0.855
4	205	0.03	0.824	0	1
5	246	0.04	1.01	0	1
6	308	0.10	1.35	0	1
7	383	0.10	1.66	0	1
8	444	0.10	1.91	0	1
9	531	0.20	2.28	0	1
10	625	0.10	2.73	0	1
11	702	0.10	3.10	0	1
12	793	0.10	3.44	0	1
13	882	0.04	3.78	0	1
14	997	0.03	4.20	0	1
15	1110	0.02	4.56	0	1
16	1226	0.01	4.93	0	1

TABLE B-7

DROP-SIZE DISTRIBUTION, SETTLING VELOCITIES v_j , REFLECTION COEFFICIENTS γ_j AND IMPACTION EFFICIENCIES ϵ_j FOR TRIAL 11 OF THE WITHLACOOCHEE SPRAY TRIALS FLORIDA, 1980

Drop-Size Category j	Mean Drop Diameter (μm)	f_j	v_j (m s^{-1})	γ_j	ϵ_j
1	51.2	0.001	0.117	0.46	0.046
2	105	0.009	0.341	0	0.194
3	150	0.02	0.585	0	0.395
4	203	0.03	0.817	0	0.726
5	262	0.04	1.12	0	1
6	335	0.10	1.46	0	1
7	420	0.10	1.81	0	1
8	491	0.10	2.10	0	1
9	604	0.20	2.64	0	1
10	719	0.10	3.14	0	1
11	788	0.10	3.40	0	1
12	877	0.10	3.73	0	1
13	966	0.04	4.06	0	1
14	1039	0.03	4.29	0	1
15	1151	0.02	4.64	0	1
16	1323	0.01	5.17	0	1

TABLE B-8
 DROP-SIZE DISTRIBUTION, SETTLING VELOCITIES v_j , REFLECTION
 COEFFICIENTS γ_j AND IMPACTION EFFICIENCIES E_j FOR
 TRIAL 13 OF THE WITHLACOOCHEE SPRAY TRIALS
 FLORIDA, 1980

Drop-Size Category j	Mean Drop Diameter (μm)	f_j	v_j (m s^{-1})	γ_j	E_j
1	50.5	0.001	0.110	0.47	0.165
2	97.5	0.009	0.294	0.01	0.339
3	145	0.02	0.543	0	0.749
4	184	0.03	0.736	0	1
5	220	0.04	0.887	0	1
6	277	0.10	1.18	0	1
7	342	0.10	1.50	0	1
8	400	0.10	1.73	0	1
9	486	0.20	2.07	0	1
10	570	0.10	2.47	0	1
11	637	0.10	2.79	0	1
12	736	0.10	3.23	0	1
13	825	0.04	3.56	0	1
14	878	0.03	3.76	0	1
15	928	0.02	3.94	0	1
16	1008	0.01	4.23	0	1

APPENDIX C
DEPOSITION PATTERNS AT THE TOP OF THE SLASH PINE CANOPY
AND BENEATH THE CANOPY

Figures C-1 through C-8 show observed and model deposition at the top of the slash pine canopy for Trials 2, 3, 5, 6, 7, 10, 11 and 13 of the Withlacoochee Spray Trials. Observed and model ground-level deposition below the slash pine canopy for these trials are shown in Figures C-9 through C-16.

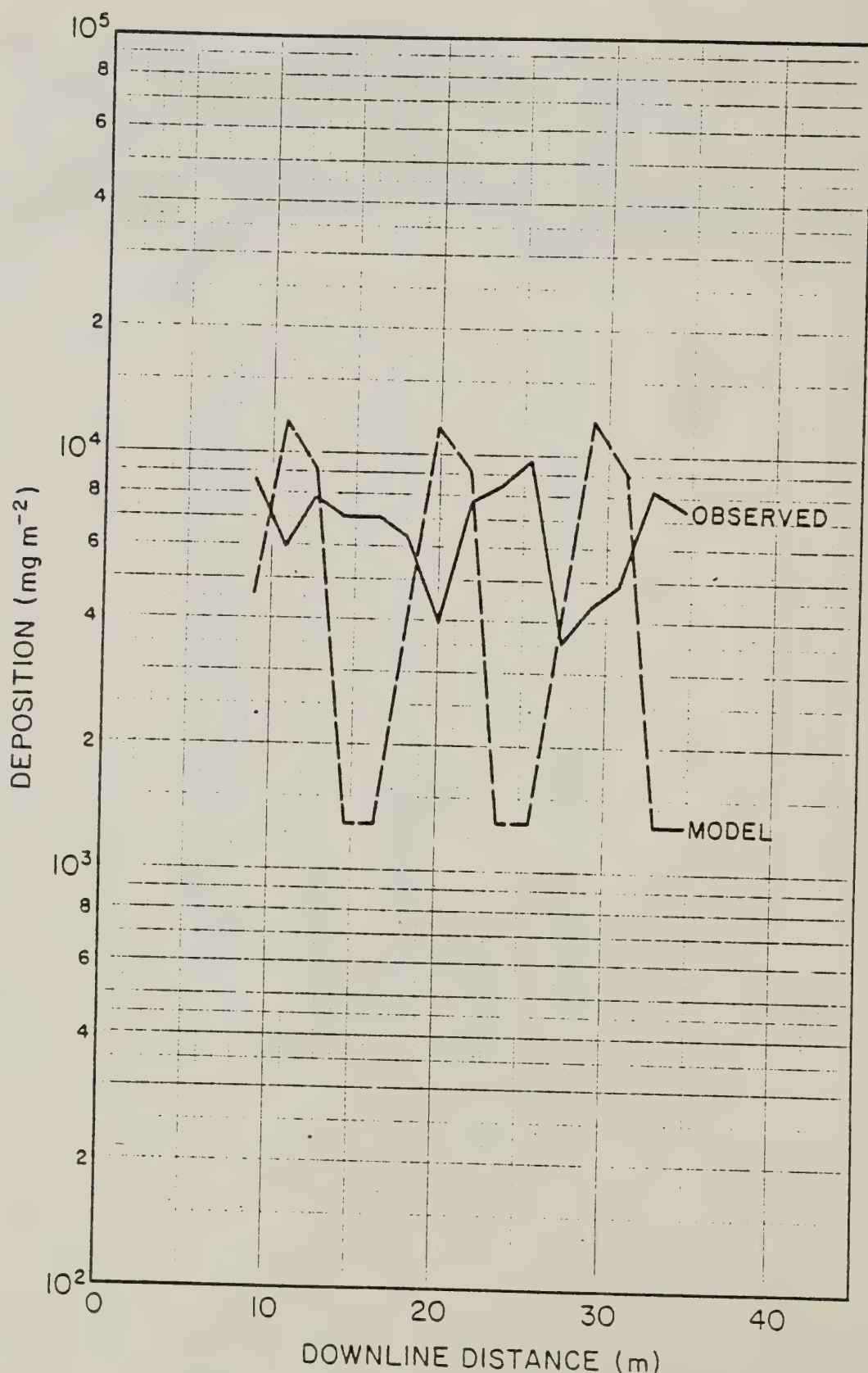


FIGURE C-1. Observed and model deposition at the top of the slash pine canopy for Trial 2, Withlacoochee Spray Trials, Florida, 1980.

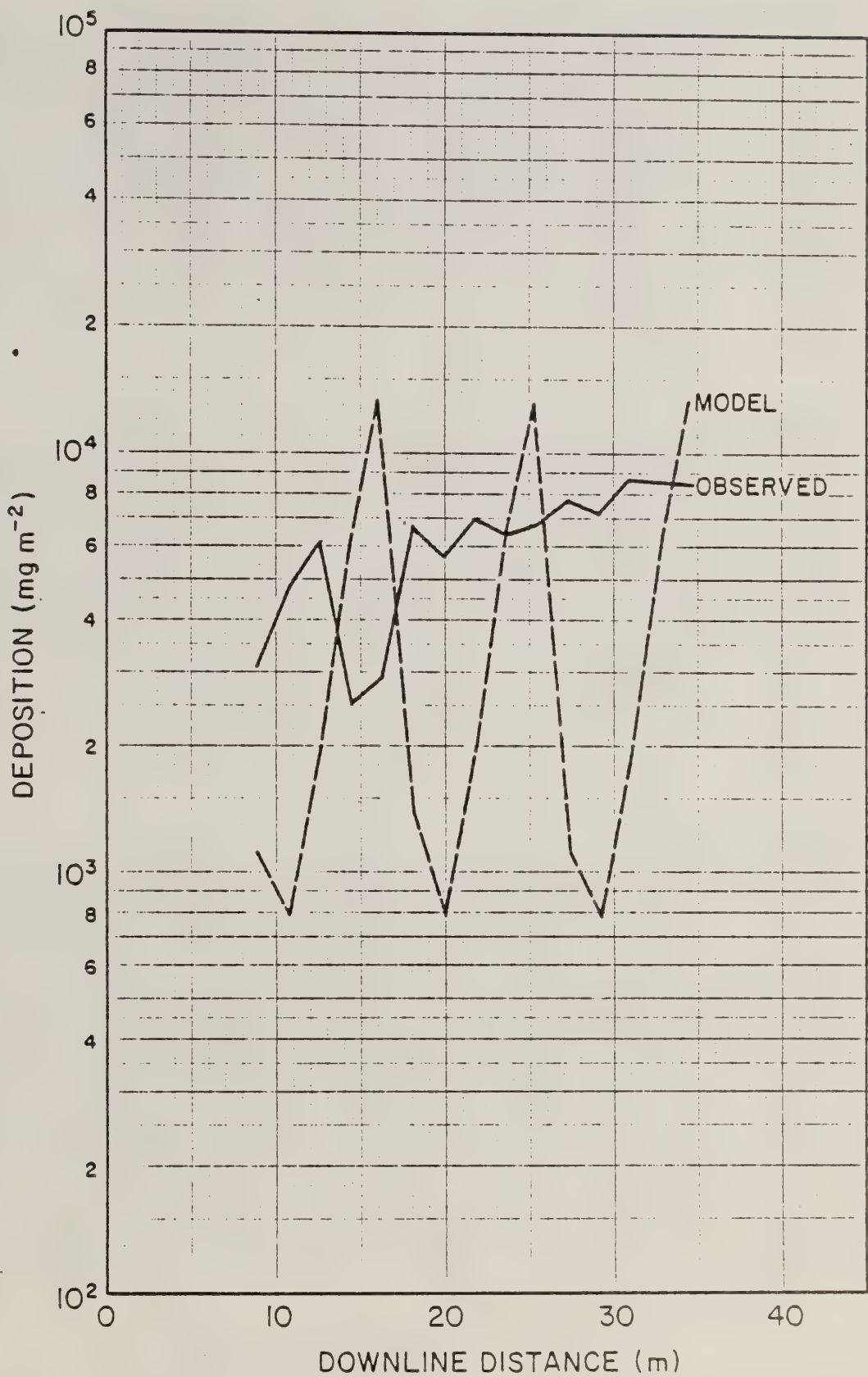


FIGURE C-2. Observed and model deposition at the top of the slash pine canopy for Trial 3, Withlacoochee Spray Trials, Florida, 1980.

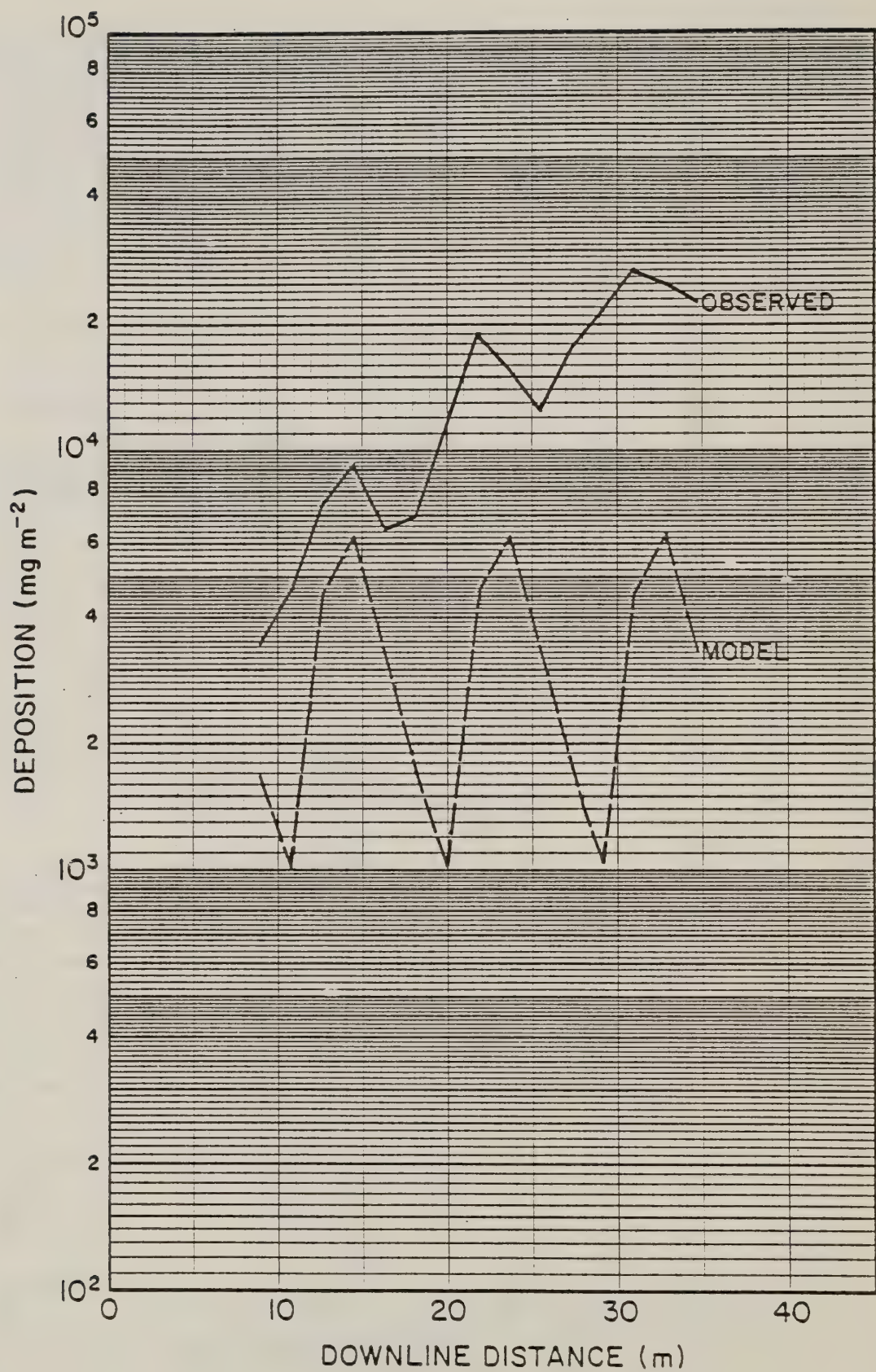


FIGURE C-3. Observed and model deposition at the top of the slash pine canopy for Trial 5, Withlacoochee Spray Trials, Florida, 1980.

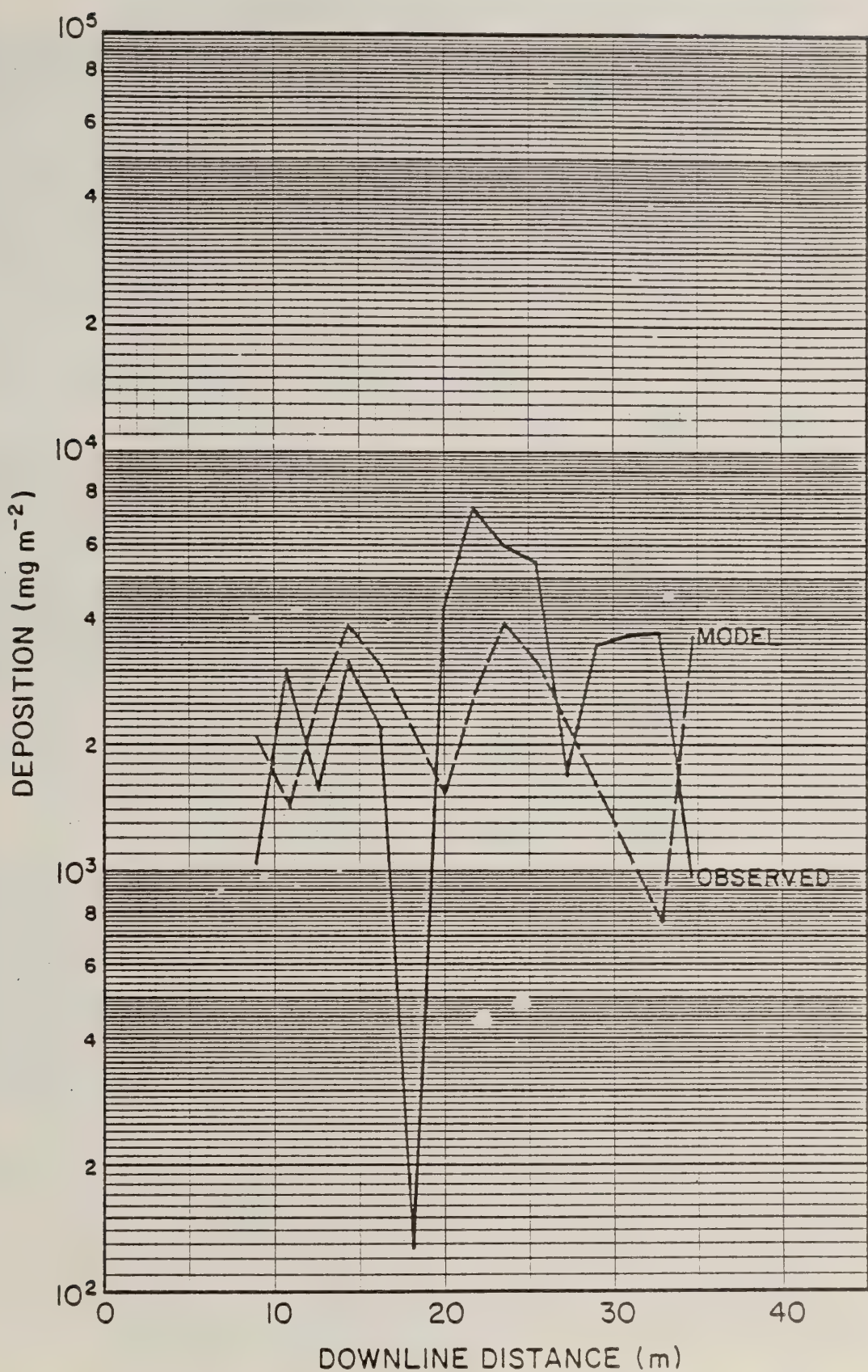


FIGURE C-4. Observed and model deposition at the top of the slash pine canopy for Trial 6, Withlacoochee Spray Trials, Florida, 1980.

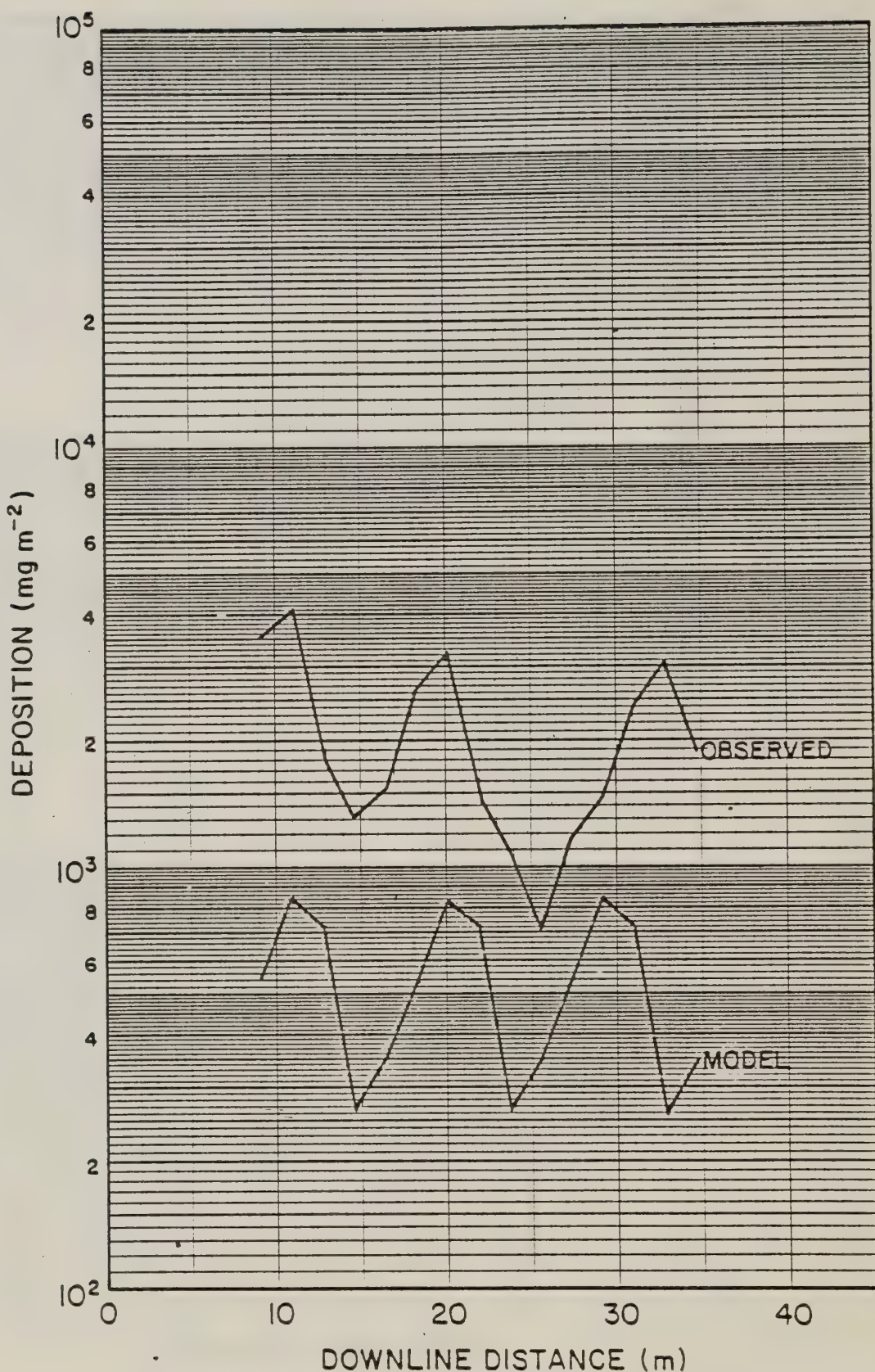


FIGURE C-5. Observed and model deposition at the top of the slash pine canopy for Trial 7, Withlacoochee Spray Trials, Florida, 1980.

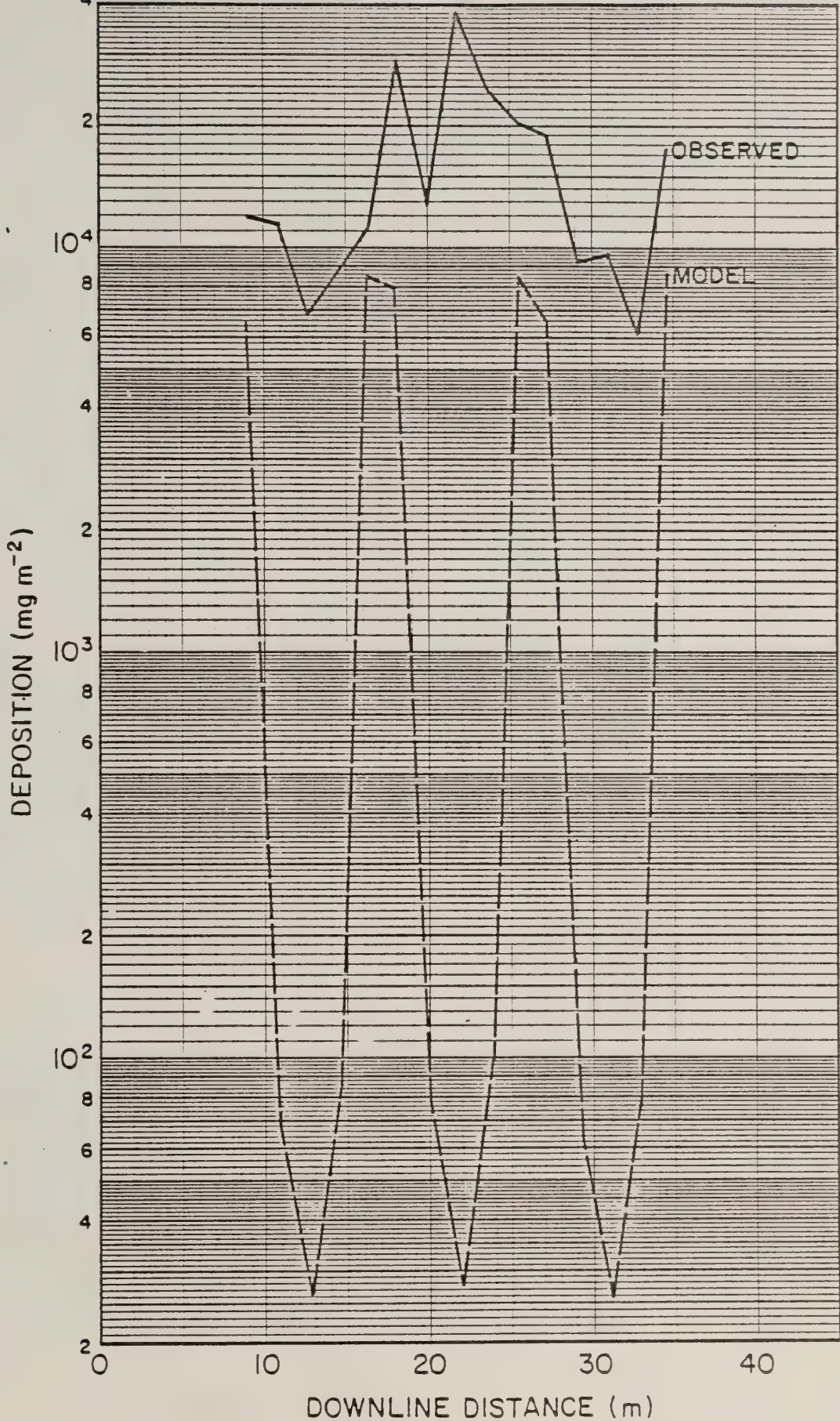


FIGURE C-6. Observed and model deposition at the top of the slash pine canopy for Trial 10, Withlacoochee Spray Trials, Florida, 1980.

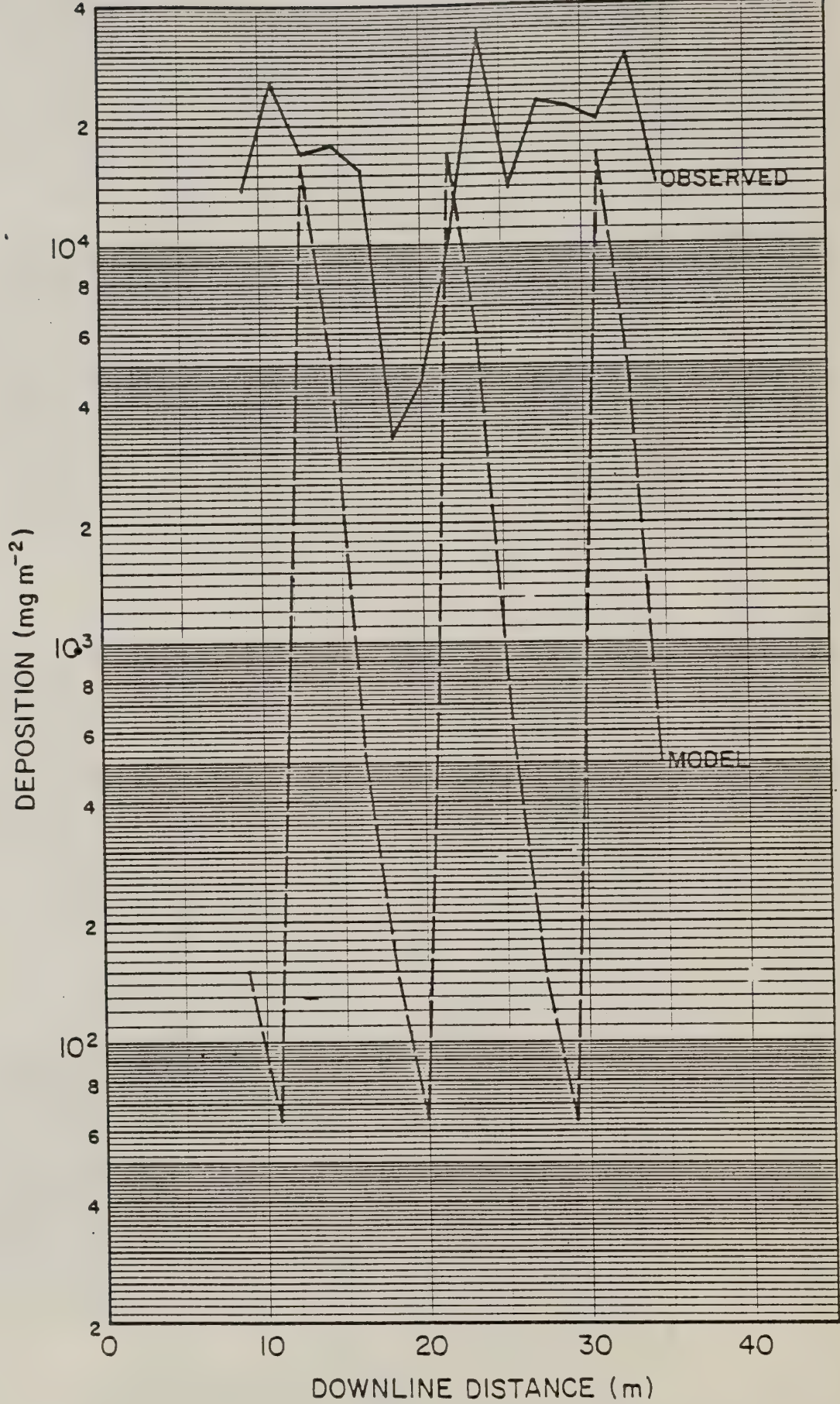


FIGURE C-7. Observed and model deposition at the top of the slash pine canopy for Trial 11, Withlacoochee Spray Trials, Florida, 1980.

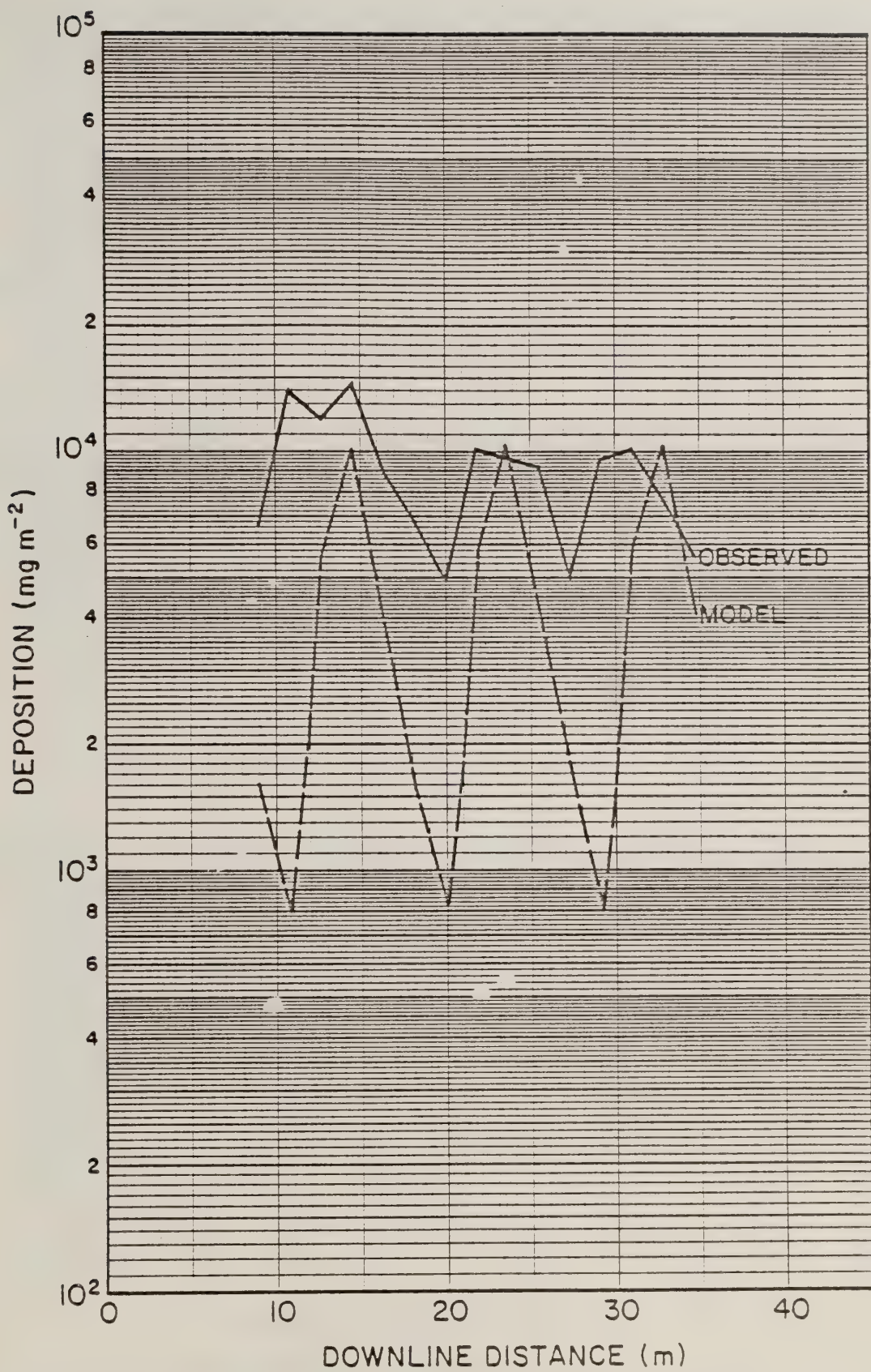


FIGURE C-8. Observed and model deposition at the top of the slash pine canopy for Trial 13, Withlacoochee Spray Trials Florida, 1980.

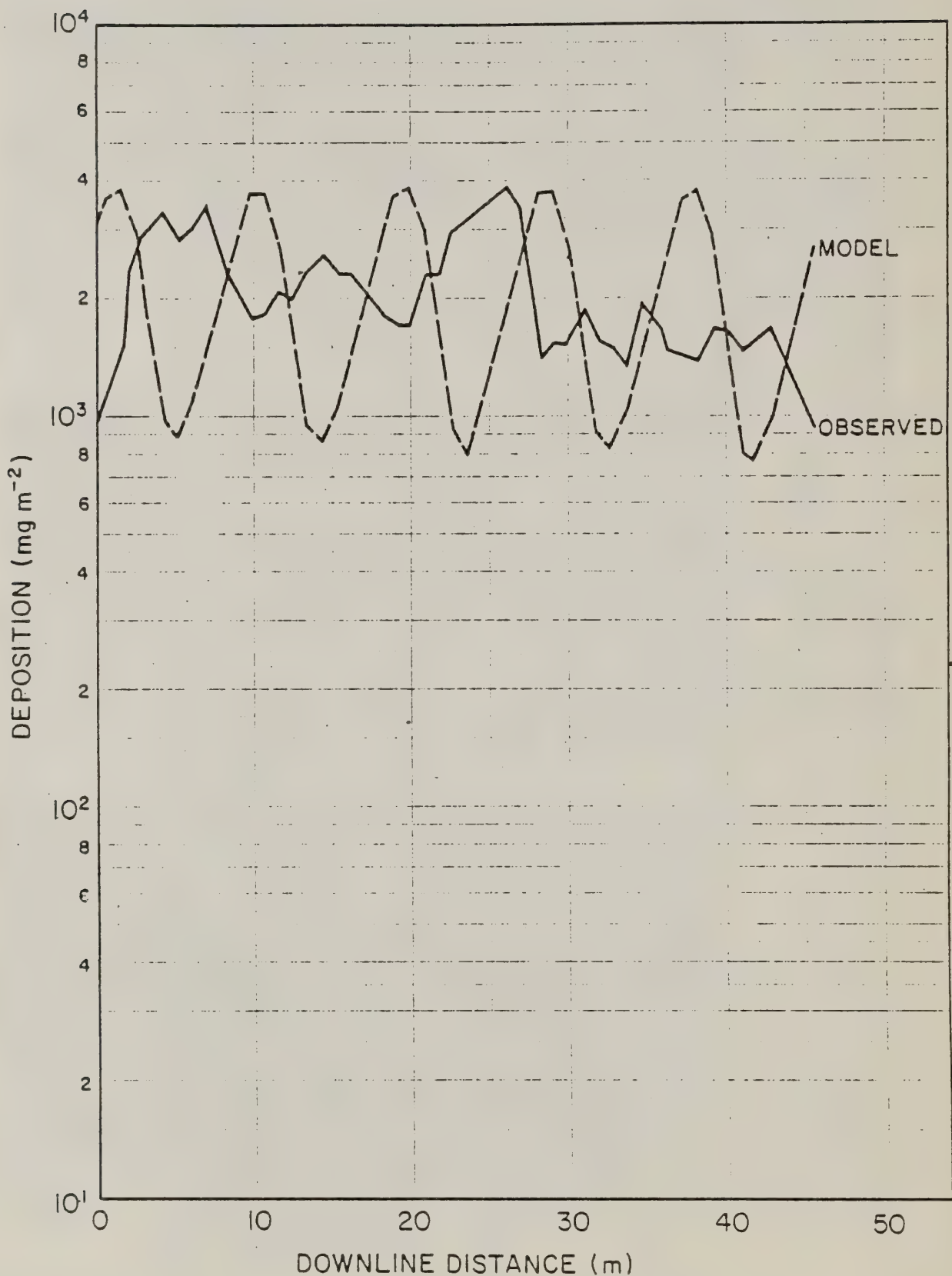


FIGURE C-9. Observed and model ground-level depositions below the slash pine canopy for Trial 2, Withlacoochee Spray Trials, Florida, 1980.

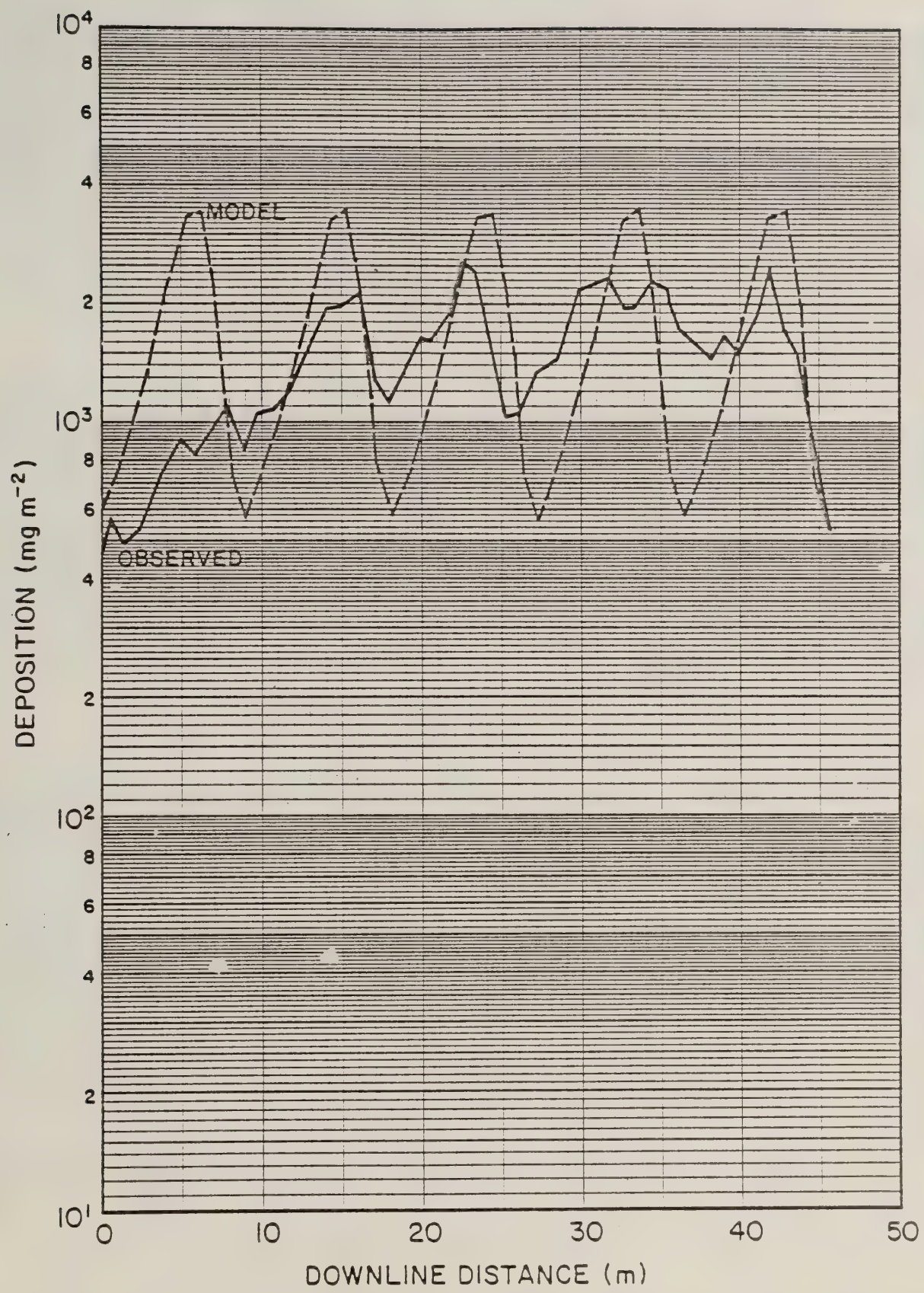


FIGURE C-10. Observed and model ground-level deposition below the slash pine canopy for Trial 3, Withlacoochee Spray Trials, Florida, 1980.

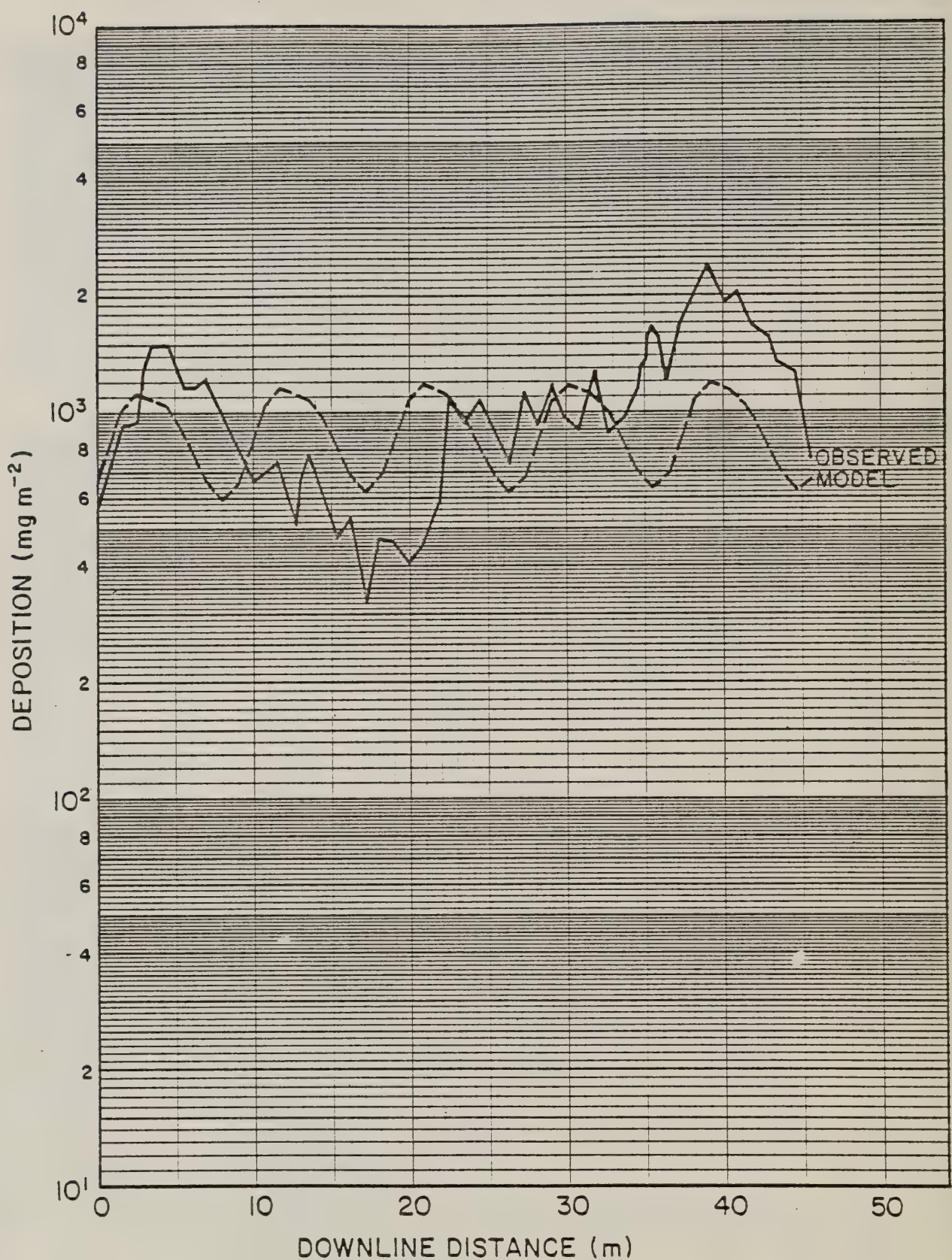


FIGURE C-11. Observed and model ground-level deposition below the slash pine canopy for Trial 5, Withlacoochee Spray Trials, Florida, 1980.

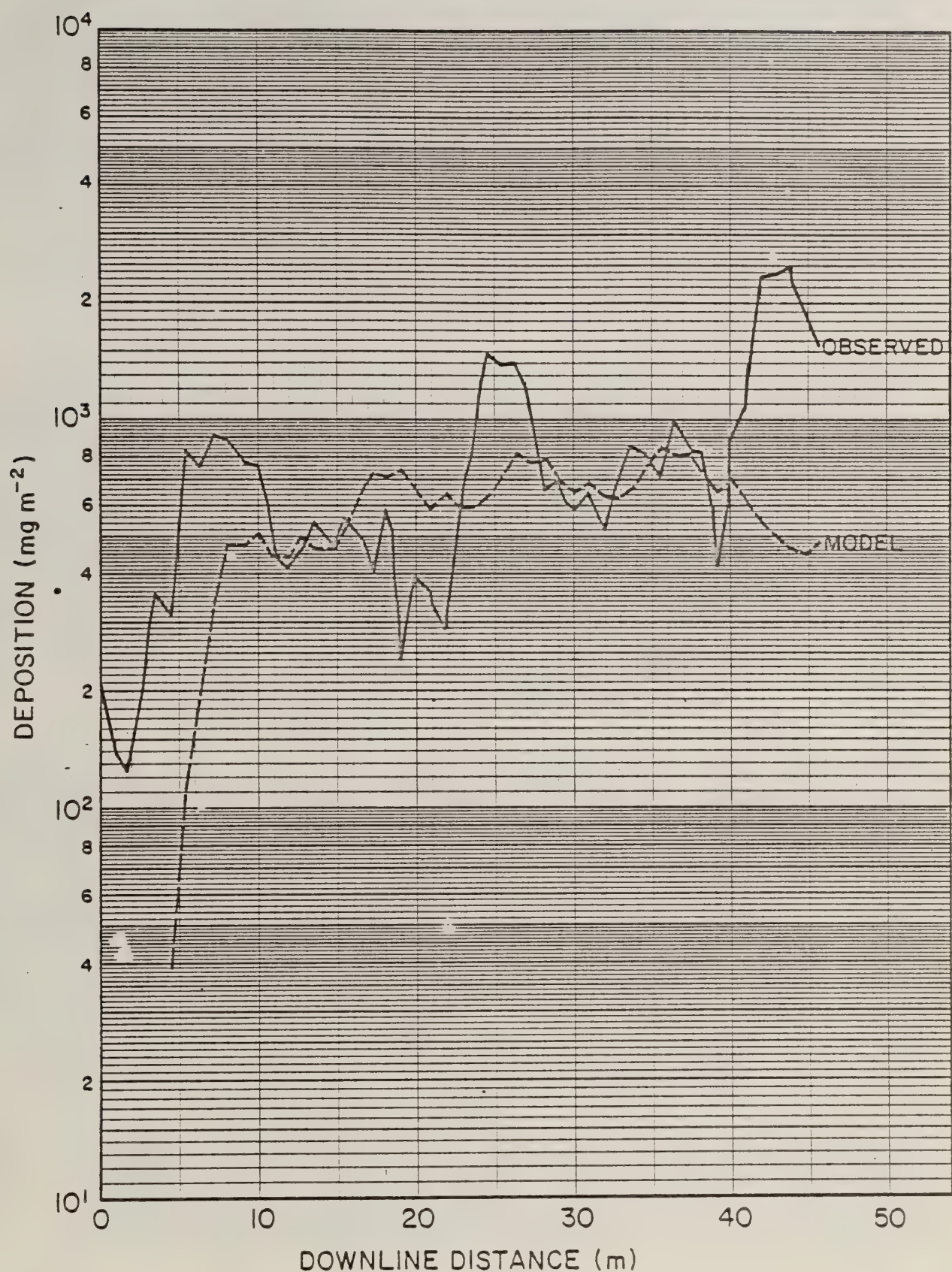


FIGURE C-12. Observed and model ground-level deposition below the slash pine canopy for Trial 6, Withlacoochee Spray Trials, Florida, 1980.

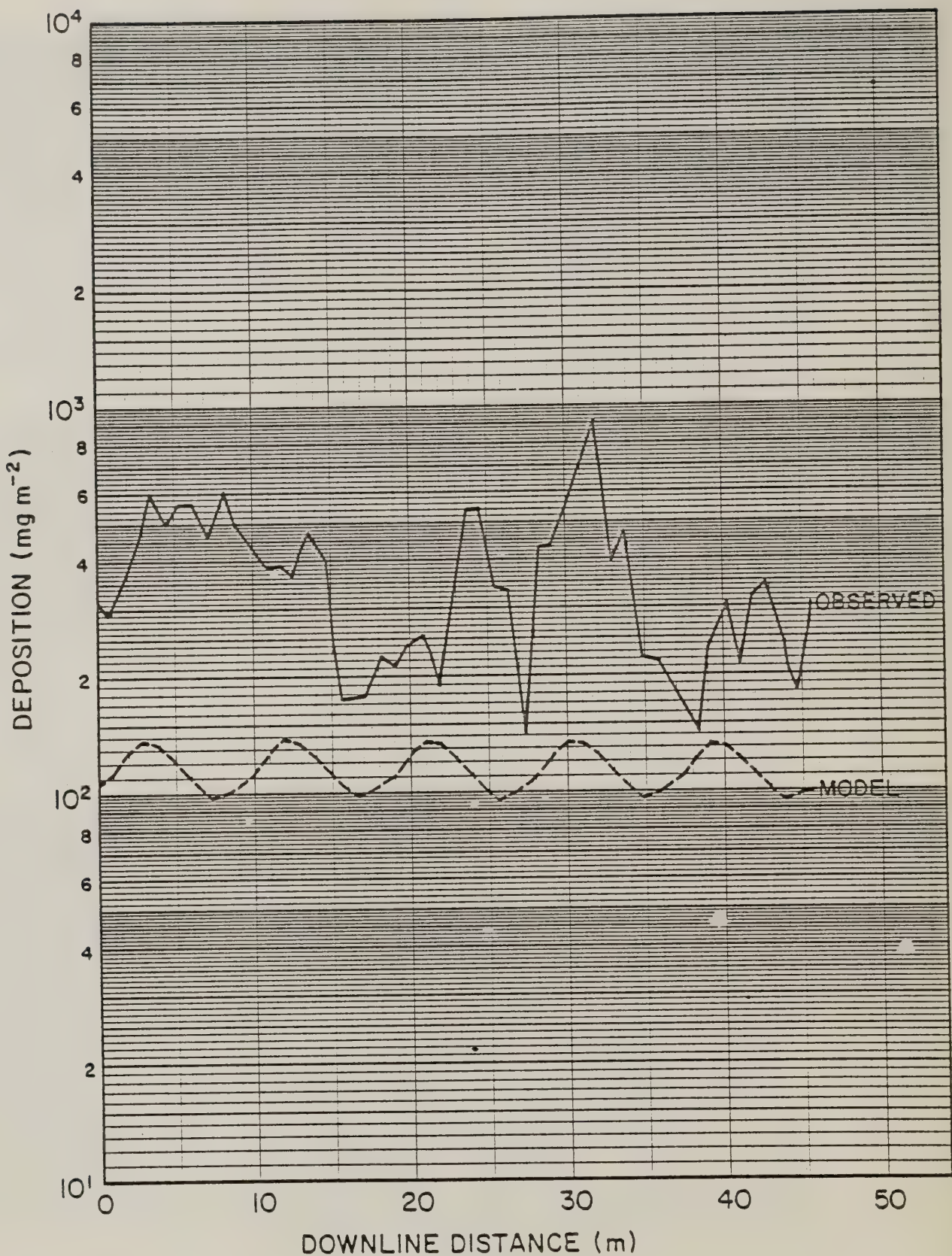


FIGURE C-13. Observed and model ground-level deposition below the slash pine canopy for Trial 7, Withlacoochee Spray Trials, Florida, 1980.

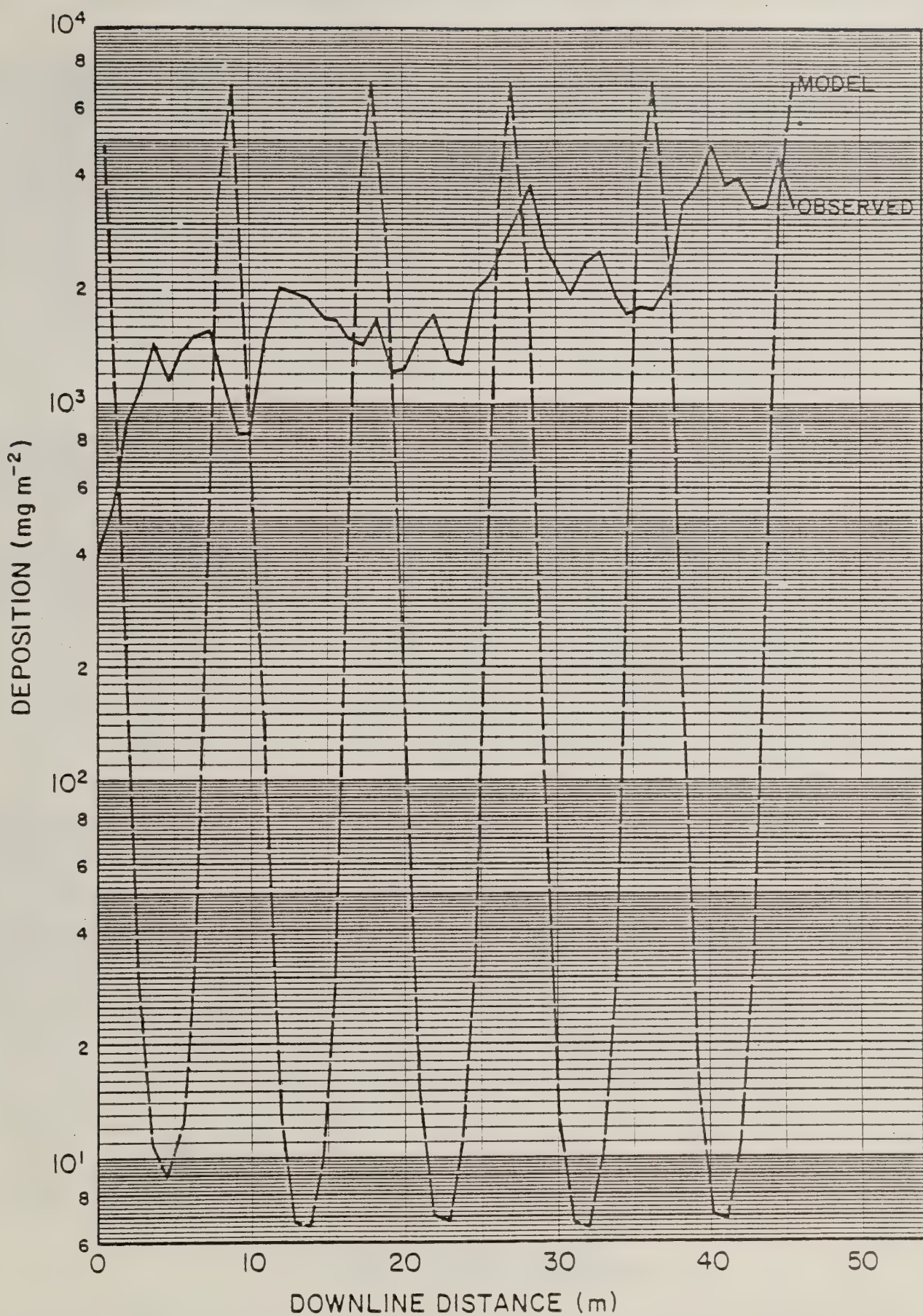


FIGURE C-14. Observed and model ground-level deposition below the slash pine canopy for Trial 10, Withlacoochee Spray Trials, Florida, 1980.

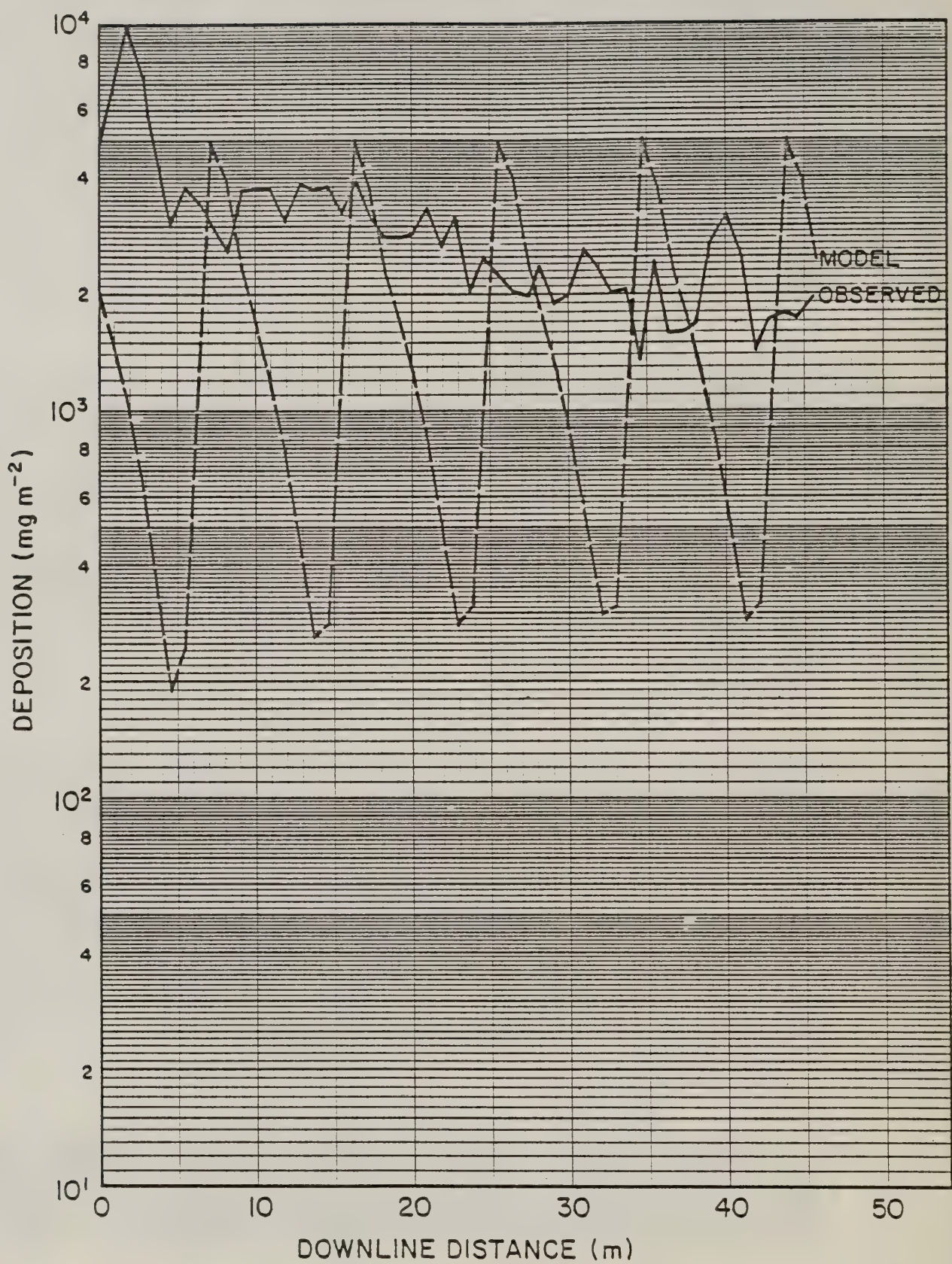


FIGURE C-15. Observed and model ground-level deposition below the slash pine canopy for Trial 11, Withlacoochee Spray Trials, Florida, 1980.

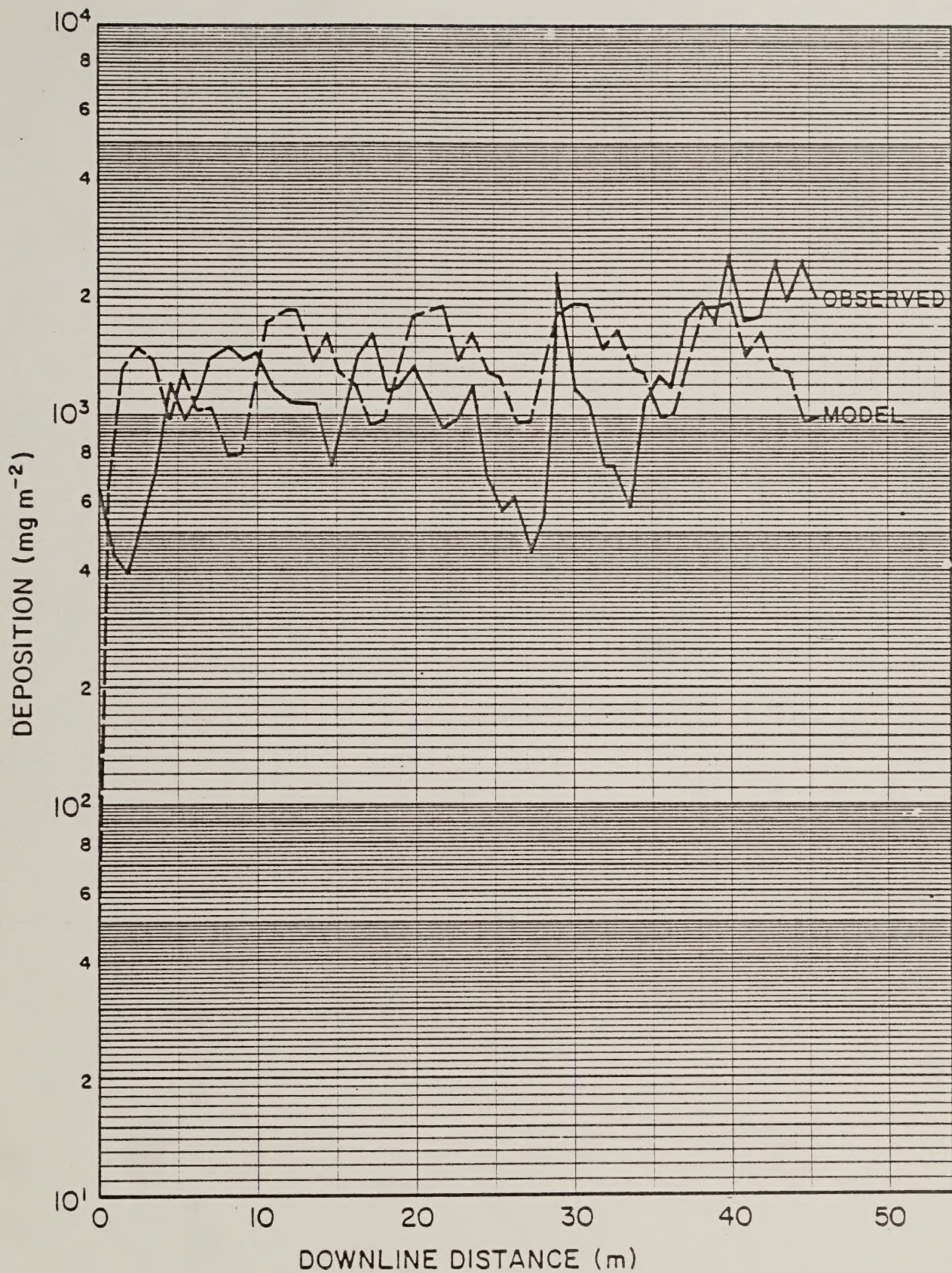


FIGURE C-16. Observed and model ground-level deposition below the slash pine canopy for Trial 13, Withlacoochee Spray Trials, Florida, 1980.

NATIONAL AGRICULTURAL LIBRARY



1023166654